~~MASTER COPY~~

IDO-17005
October 1964

95,546

~~48~~

THE ADVANCED REACTIVITY MEASUREMENT FACILITIES
A Description and Performance Evaluation

MASTER

E. E. Burdick, E. Fast, and D. W. Knight

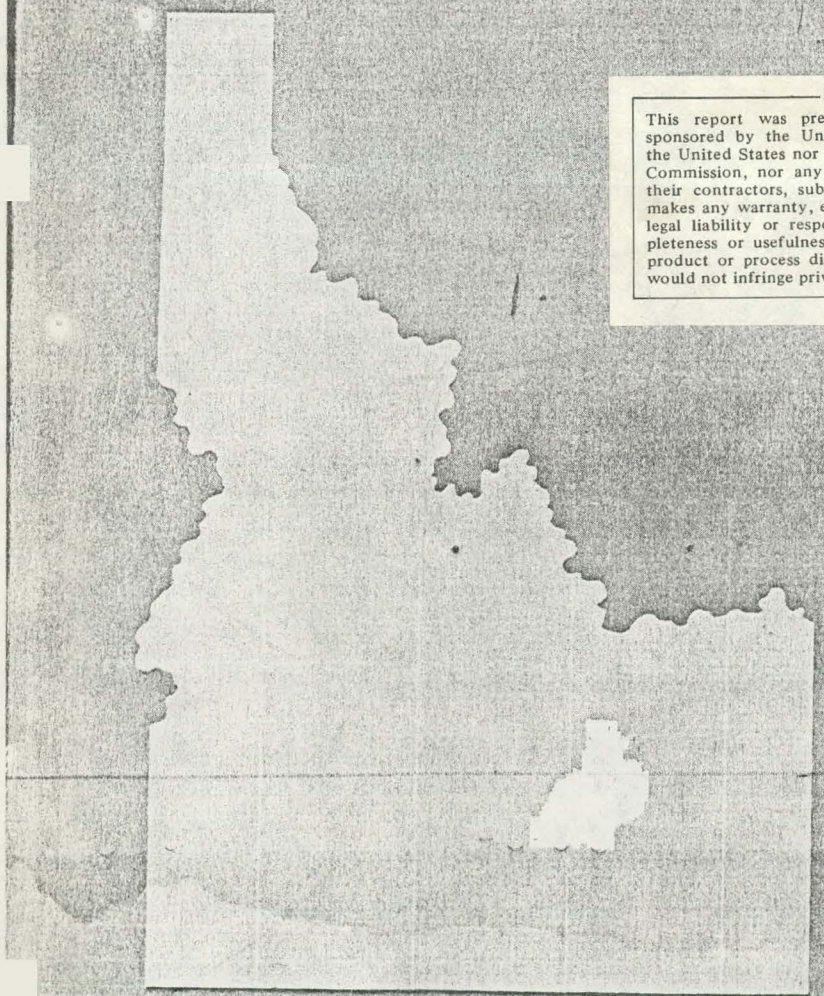

PHILLIPS PETROLEUM COMPANY

PHILLIPS 66

ATOMIC ENERGY DIVISION

NATIONAL REACTOR TESTING STATION
US ATOMIC ENERGY COMMISSION

DISCLAIMER

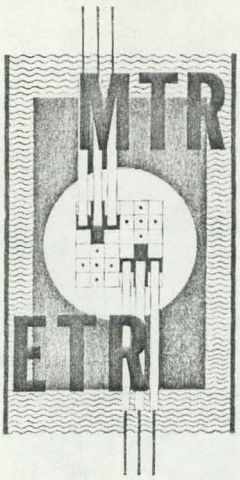

IDO-17005
AEC Research and Development Report
Reactor Technology
TID-4500 (34th Ed.)
Issued: October 1964

THE ADVANCED REACTIVITY MEASUREMENT FACILITIES
A Description and Performance Evaluation

by

E. E. Burdick
E. Fast
D. W. Knight

PHILLIPS
PETROLEUM
COMPANY

Atomic Energy Division
Contract AT(10-1)-205
Idaho Operations Office
U. S. ATOMIC ENERGY COMMISSION

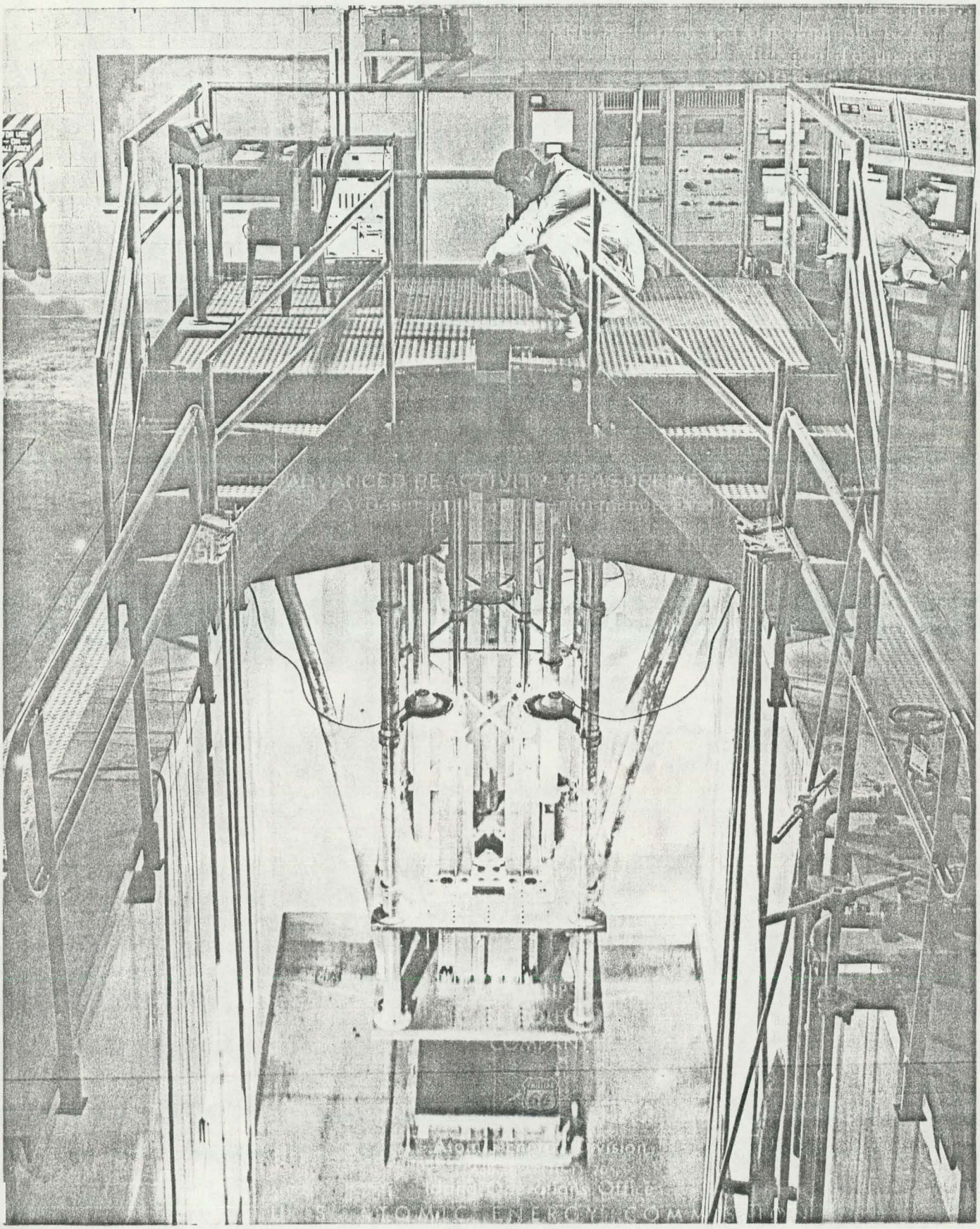

ABSTRACT

The Advanced Reactivity Measurement Facilities, ARMF-I and ARMF-II, are nearly identical critical facilities and are used almost exclusively for measuring reactor physics parameters, such as reactor-spectrum cross sections and resonance integral cross sections. They are, therefore, designed to (a) have large statistical weights for fuels and poisons, (b) be mechanically stable enough to produce reproducible reactivity measurements, and (c) have sensitive instrumentation capable of measuring very small reactivities. These facilities are swimming-pool-type reactors having light-water moderated cores made up of plate-type fuel elements containing fully enriched U-235. The facilities are located at the National Reactor Testing Station in Idaho near the Materials Testing Reactor (MTR). Being located near the MTR permits measurements on short-lived fission products and transmuted isotopes. By use of the capsule transfer tube connecting the MTR and ARMF canals, a capsule can be transferred from the MTR hydraulic rabbit to the ARMF and prepared for reactivity measurements in 15 minutes.

Both ARMF reactors use a servo-controlled regulating rod for reactivity measurements rather than a pile oscillator. The reactivity effect of a capsule placed in the reactor is determined from the resultant regulating rod displacement. In order to make the regulating rod a precise measuring device, its drive and position instrumentation includes no gears. Because the rod rotates about a vertical axis, it can be driven by a torque motor, the armature of which is attached directly to the rod. A digital shaft-angle encoder, the position transducer, also attaches directly to the rod.

Characteristics important to facilities used for reactivity measurements are statistical weights and expected measurement errors. Typical statistical weights in the ARMF are (a) 2.8×10^{-2} $\Delta k/k$ per g of natural boron, (b) 6.36×10^{-4} $\Delta k/k$ per g of U-235, and (c) 1.16×10^{-4} $\Delta k/k$ per g of gold inside a cadmium shield. Expected measurement error (standard deviation) for a single 4.5 minute capsule measurement is 10^{-7} $\Delta k/k$.

ACKNOWLEDGMENTS

The information in this report is based on the work of many people. The ARMF design criteria were set forth by D. R. deBoisblanc after conferring with Argonne and Westinghouse-Bettis personnel. Instrumentation and mechanical design were carried out by Phillips' Instrument Development and Design Engineering Branches, respectively.

TABLE OF CONTENTS

FIGURES

TABLES

THE ADVANCED REACTIVITY MEASUREMENT FACILITIES (ARMF-I AND ARMF-II)

A DESCRIPTION AND PERFORMANCE EVALUATION

The Advanced Reactivity Measurement Facilities (ARMF-I and ARMF-II) are nearly identical critical facilities used almost exclusively for measuring reactor physics parameters such as reactor-spectrum cross sections and resonance integral cross sections. Since ARMF-I and -II are sequels to the Reactivity Measurement Facility (RMF) [1, 2, 3], it is appropriate to introduce this report with some background information on the RMF. The report then describes the physical and nuclear aspects, and the control system of the ARMF. Also included is an experimental evaluation of the precision of ARMF reactivity measurements. Since the two reactors are nearly identical, the singular will be used to describe components that are the same in both reactors; only when differences exist will the two reactors be described separately.

I. BACKGROUND

It was recognized early in the operation of the Materials Testing Reactor (MTR) that it would be valuable to have nearby an instrument capable of nondestructively measuring the changes in poison and fuel concentrations in a capsule (sample) after high neutron flux irradiations. Thus, it was proposed that this instrument be a zero power nuclear reactor which would also be capable of measuring other reactor physics parameters, such as reactor-spectrum cross sections and resonance integrals. This proposal led to the construction of the Reactivity Measurement Facility (RMF) which first became critical on February 11, 1955. In order that capsule transfers between the MTR and RMF could be made conveniently and quickly, the RMF was located in the MTR canal. Also, because the value of the RMF could only be estimated at that time, the resultant cost savings of not constructing a new canal and building was a significant consideration in locating the RMF.

At the time the RMF was built, other reactors making reactivity measurements used the danger-coefficient method or the more preferred pile-oscillator method. It is noted that the pile oscillator has an open-loop feature which usually presents drift or instability problems not encountered in a closed loop system. In order to take advantage of the closed loop feature, a servo-controlled regulating rod was included in the RMF. After calibrating the regulating rod, the reactivity worth of a capsule is obtained directly from the resultant displacement of the rod when a capsule is placed in an experimental core position. Even a servo-controlled reactor is susceptible, however, to reactivity drifts caused by temperature fluctuations and mechanical instability of the core. RMF experience showed that these effects made it desirable to make measurements of the reference conditions between each capsule measurement. Drifts in the servo-controlled rod position instrumentation also contributed to apparent reactivity drifts. In order to provide a convenient means for making the reference measurements, a capsule oscillator[a] was installed.

Because demands for operating time exceeded the time available, a second reactor was constructed. This reactor was built with improvements based on RMF experience; therefore, it was designated the Advanced Reactivity Measurement Facility (ARMF). The ARMF design included features to minimize the effects which cause reactivity drifts.

In the hope of eliminating the need of frequent reference measurements and, thus, the capsule oscillator, the ARMF was placed in its own canal to avoid the temperature fluctuations experienced in the MTR canal. The core was made as mechanically stable as feasible, and the servo-controlled rod position instrumentation was changed from an analog to a digital system. The desired feature of rapid transfer of capsules from the MTR to the ARMF was retained by placing a hydraulic capsule-transfer tube between the two canals. In spite of these improvements, provisions were made, however, for installing an oscillator in case it is needed or becomes desirable for situations not considered.

Although the ARMF building and canal were made large enough to house the RMF also, the latter facility was never moved. Instead, the RMF was dismantled

---

[a] The term capsule oscillator, rather than pile oscillator, is used here because the pile power is held constant in the RMF by the servo controlled regulating rod.

and a second ARMF was built because of the improvements that had been realized with the original ARMF and the cost of moving and modifying the RMF. (Modifications to the RMF would have been required to improve its safety as well as improve its precision.) The two ARMF reactors were designated ARMF-I and ARMF-II according to the chronology of their origin. The two ARMF reactors became critical on October 3, 1960 and December 14, 1962, respectively. The RMF was dismantled in April 1962.

II. BUILDING AND CANAL

ARMF-I and ARMF-II are housed in a 40-foot by 60-foot cinder block building located just east of the MTR canal tunnel (Figure 1). This location provided convenient connection of the MTR and ARMF canals with a capsule transfer tube. As shown in the floor plan of Figure 2, the building and canal were designed to accommodate two reactors and their control systems, sample preparation, instrument repair, and equipment storage. In addition, the building contains a 5-ton capacity crane which is used for handling miscellaneous heavy objects and makes possible the transfer of radioactive capsules in casks as an alternative to using the hydraulic capsule-transfer tube.

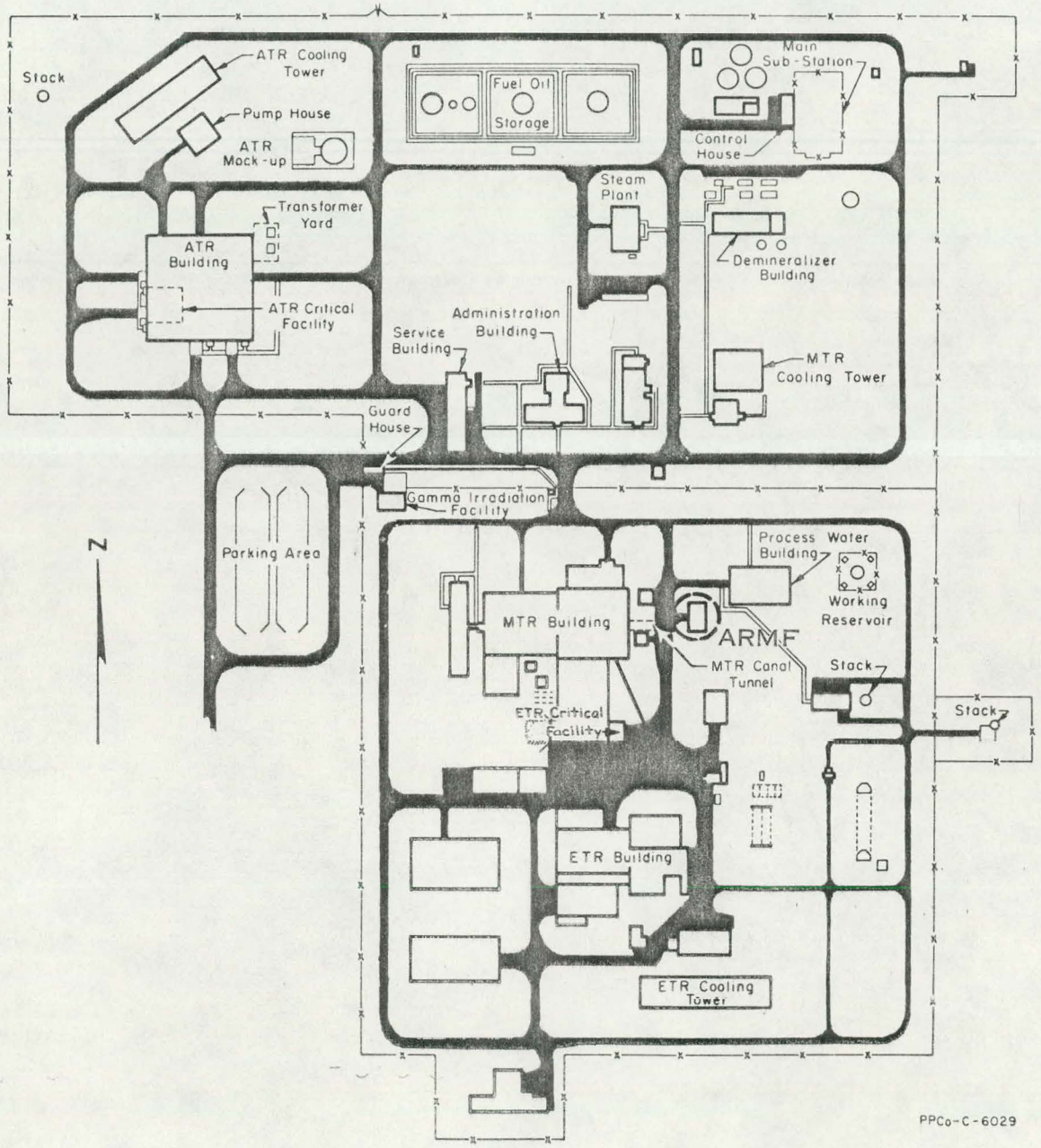

Fig. 1 Test Reactor Area (TRA) plot plan.

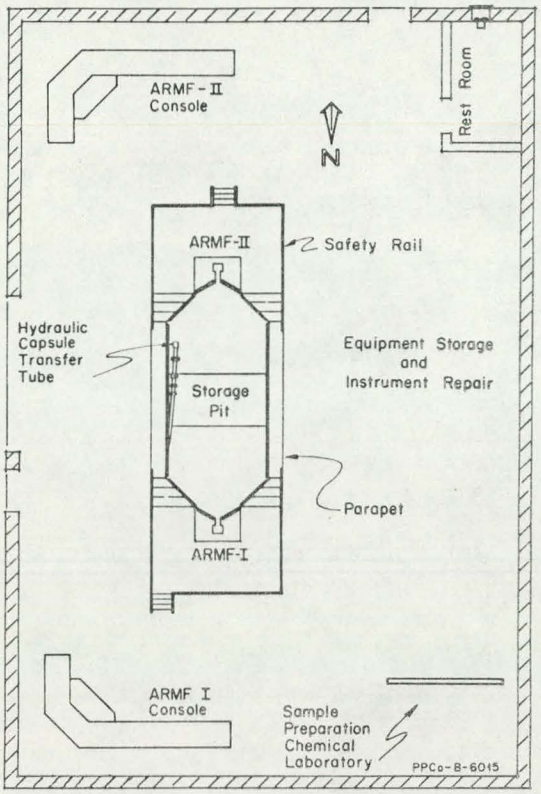

Fig. 2 ARMF building floor plan.

The canal is a monolithic concrete tank, 28 feet long, 8 feet wide, and 18 feet deep. A storage pit at the center of the canal extends the depth an additional 5 feet. Slots at two places in the canal wall permit the insertion of bulkheads to permit the draining of either end, independently if necessary, for individual reactor servicing. A general view of the canal area is shown in the photograph of Figure 3 and a cross sectional view in Figure 4.

The hydraulic capsule-transfer tube, the arrangement of which also is shown in Figure 4, uses plant demineralized water for pressure. The shuttle will accommodate capsules as large as 2-1/8 inch diameter and 10-1/8 inch long. It is possible by use of this tube to get a capsule from the MTR into the ARMF in 15 minutes if the capsule is irradiated in an MTR hydraulic rabbit facility.

The temperature of the canal water is controlled by manual manipulation of the demineralized water purge rate, normally 1 to 6 gpm, and by the number of underwater illuminating lights. On rare occasions, steam is injected to achieve a rapid temperature rise. The temperature is controlled to an accuracy of ± 0.005°C during operating periods with little operator effort. Since control is manual, temperatures outside these limits are occasionally experienced during nonoperating periods. However, during reactor start-up the temperature can be brought back to the control point of 18°C, which, except for special experiments, is the normal control temperature. The continuous water purge also prevents water stagnation and murkiness.

Equipment provided in the canal includes three trays (two of which are adjustable in height) for handling capsules, loading flux monitor wires, etc. A hydraulically operated vise is mounted on one of these trays for convenience in working with activated capsules.

The sample preparation area consists of a hood, laboratory sink, storage cabinet, and laboratory table as shown in the photograph of Figure 5. The hood is equipped with an exhaust fan and an absolute filter for safe handling of alpha-emitting isotopes. The usual laboratory utilities are provided.

The ventilation system, depending on the outside temperatures, supplies the building with up to 8500 cubic feet/minute of outside air. The building has a pressure-regulated exhaust system which maintains a positive pressure of approximately 0.1 inch of water. This feature minimizes the infiltration of dust through doorways and cracks.

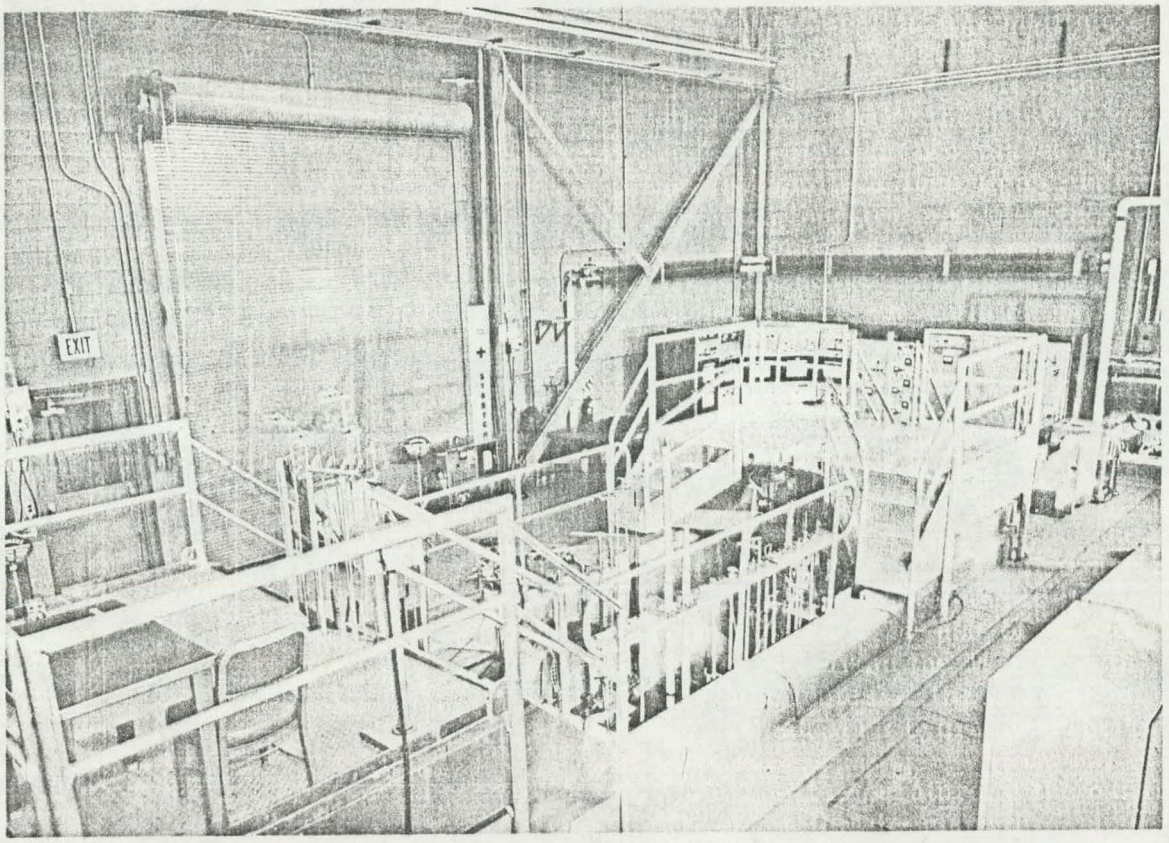

Fig. 3 ARMF canal area.

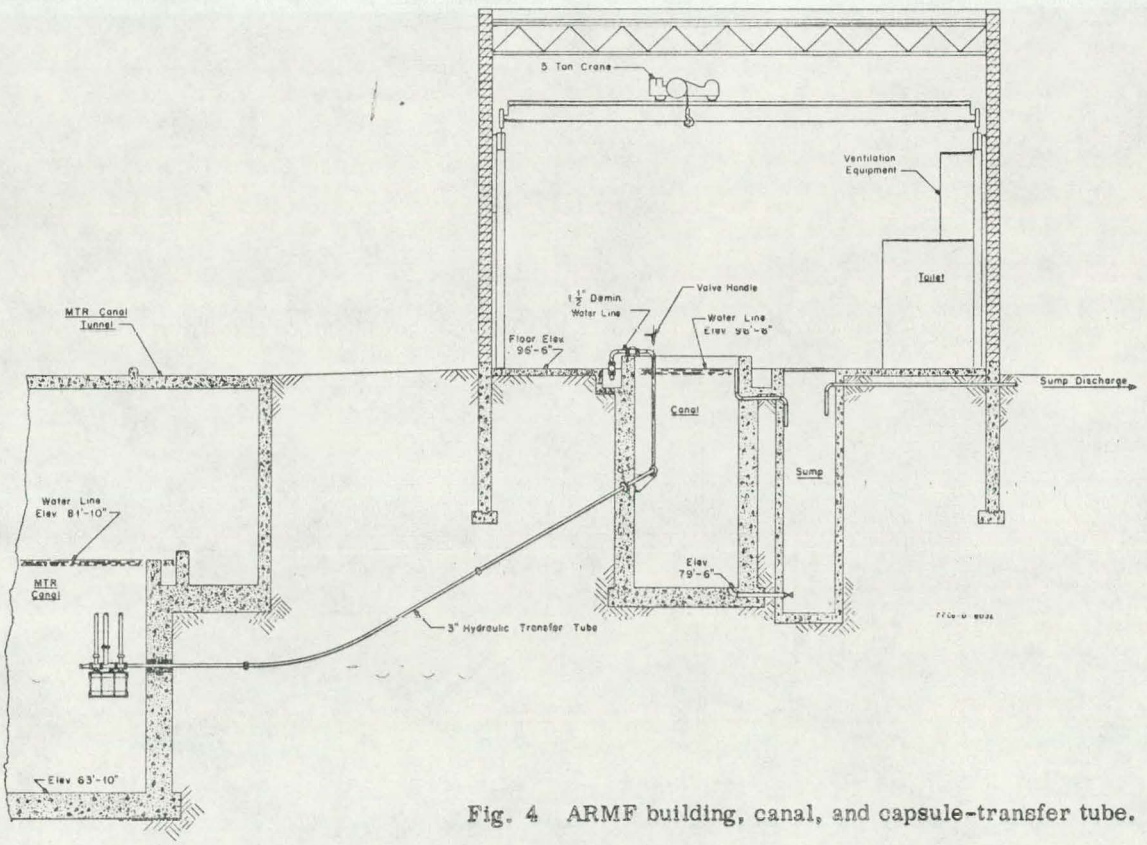

Fig. 4 ARMF building, canal, and capsule-transfer tube.

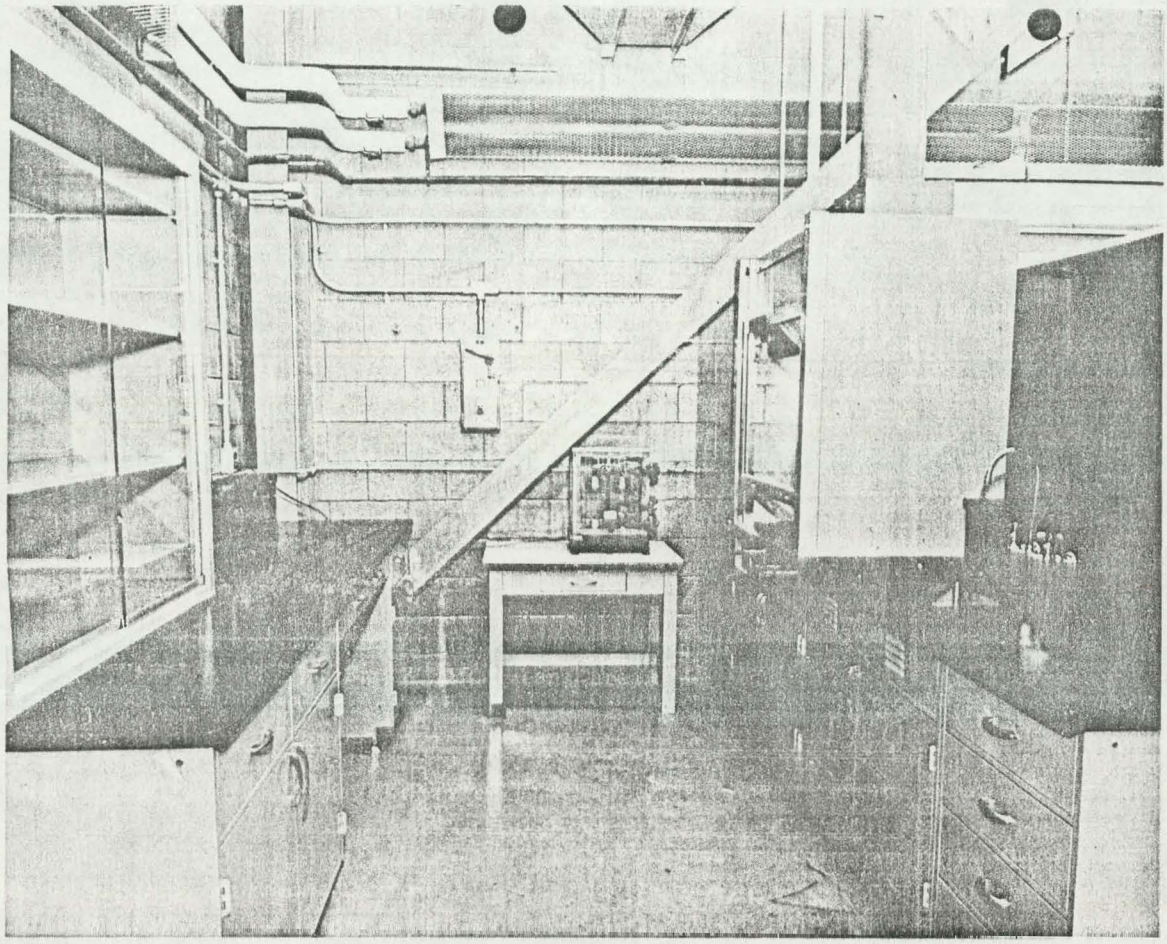

Fig. 5 ARMF sample preparation area.

III. REACTOR DESIGN

1. REACTOR STRUCTURE

The reactor structure (Figure 6) consists of a control bridge, lattice support frame, and upper and lower grid plates. These components are assembled to form a single unit which rests on the canal parapet.

The control bridge is a grid-work of steel I-beams and channels covered, top and bottom, with steel plates. It is roughly U-shaped so that capsules are easily transferred from canal storage to the core by means of handling tools or attached strings. Openings are provided in the bridge for access to instrument thimbles. The safety and control rod drives are mounted and the instrument thimbles are terminated on the control bridge.

The lattice support frame, a tubular structure, is attached to the bottom side of the control bridge. It supports the lattice through attachments at the four corners of the upper grid plate.

The upper and lower grids are two 46-inch-square, aluminum plates spaced by spindles at the four corners. These grids have penetrations for accommodating a 6 x 6 array of fuel assemblies, six instrument thimbles in ARMF-I and seven in ARMF-II, four safety rods, a shim rod, a regulating rod, a central water hole capsule holder, and miscellaneous reflector experiments. The upper and lower grids are 2 inches and 3 inches thick, respectively. In order to provide access to the fuel elements, the upper grid was made with four removable sections (Figure 7). Stainless steel pins position these sections to an accuracy of $\pm$ 0.0004 inch. Both grids have stainless steel fuel-element, grid-adaptors (Figures 8 and 9) which hold and position the fuel elements. These adaptors are bolted and taper-pinned to the grid plates for accurate and permanent positioning. The fuel-element, grid-adaptors are built to very close tolerances and, therefore, confine the fuel elements to their designated position very accurately. A counter sink provides almost exact horizontal positioning, and slots into which two pins on the element fit provide rotational positioning accurate to $\pm$ 0.0006 inch at the perimeter of the element. The adaptors on the lower grid are composed of one piece; whereas those on the upper grid are, in effect, composed of two concentric cylinders plus a coil spring. This spring loads the upper end of the fuel elements, which ensures a fit between the fuel element and the grid adaptor. The sliding fit of the two cylinders is 0.004 inch, and lateral movement is minimized by a horizontal loading device, which consists of two ball bearings and a spring clip.

To isolate the core from external vibrations, a fiber-glass vibration absorber pad separates the control bridge from the parapet. (Measurements which confirm the effectiveness of the pad are presented in Appendix A.) An auxiliary structure which also protects the core from external vibration or mechanical shock is the working platform. This platform is a bridge on which operating personnel stand to make capsule or core changes in the reactor. It spans and surrounds the control bridge and rests upon the building floor. The opening in the platform deck through which capsules are changed is small so that capsule handling tools do not come in contact with the reactor structure.

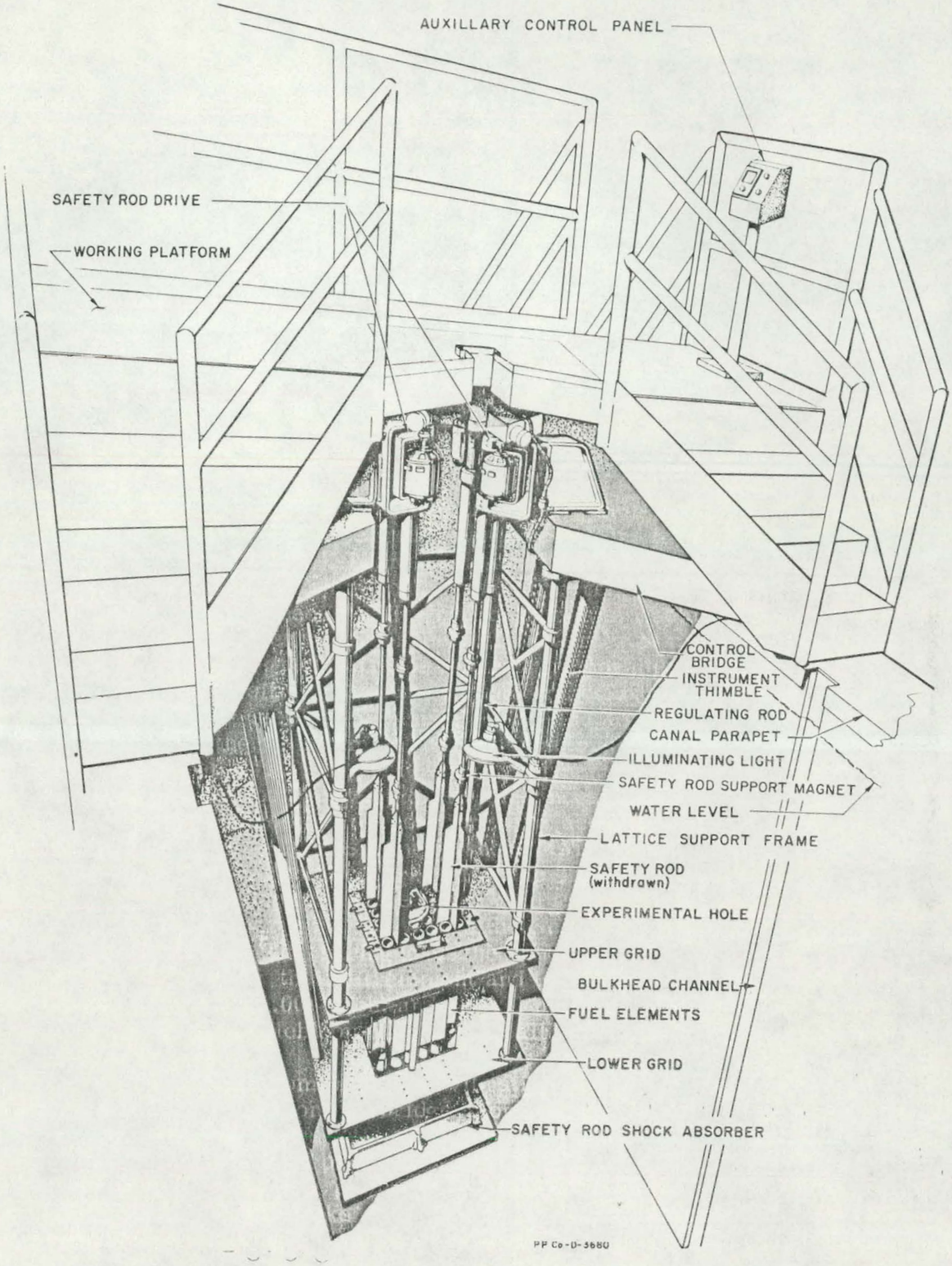

Fig. 6 ARMF reactor structure.

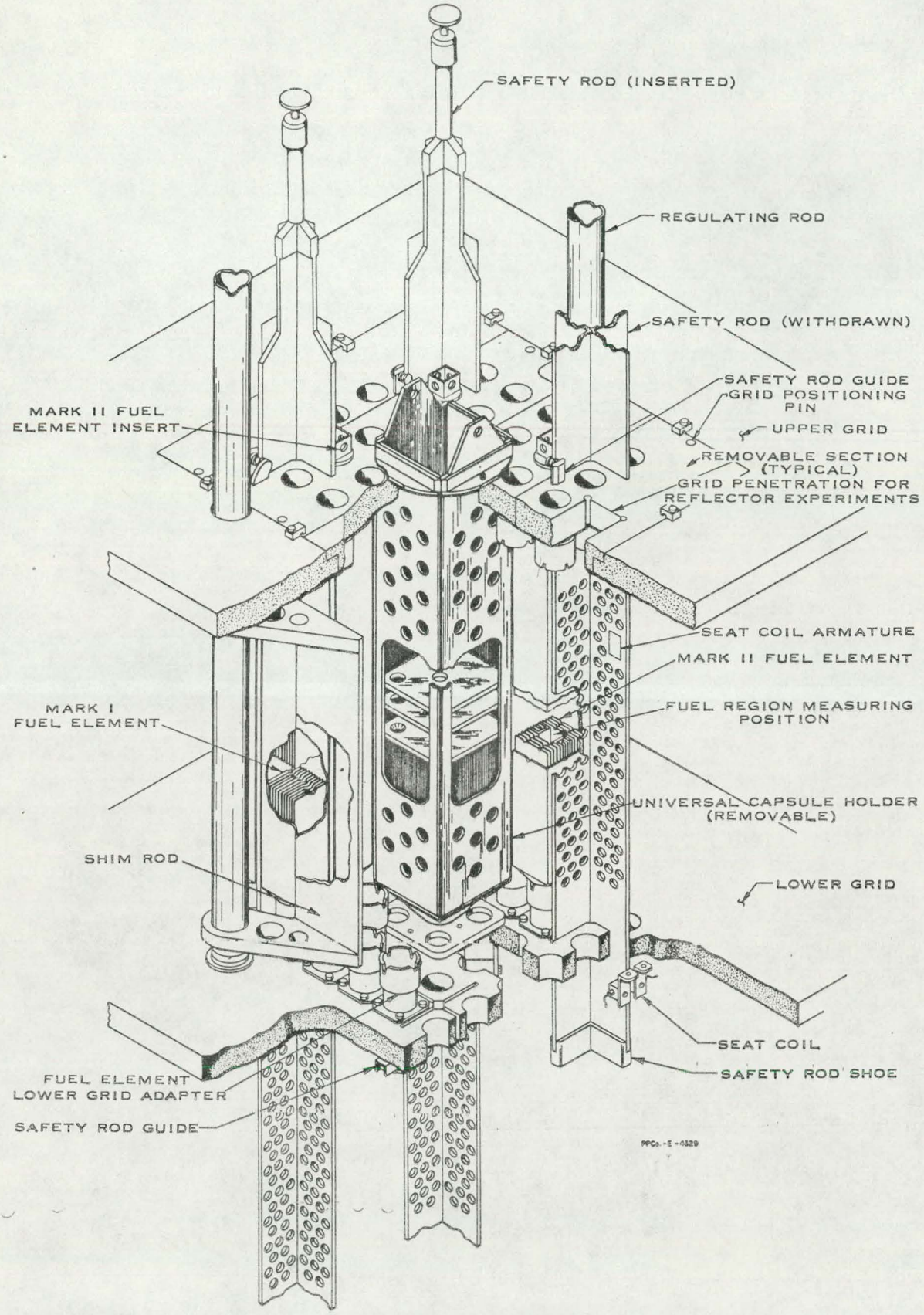

Fig. 7 ARMF core structure.

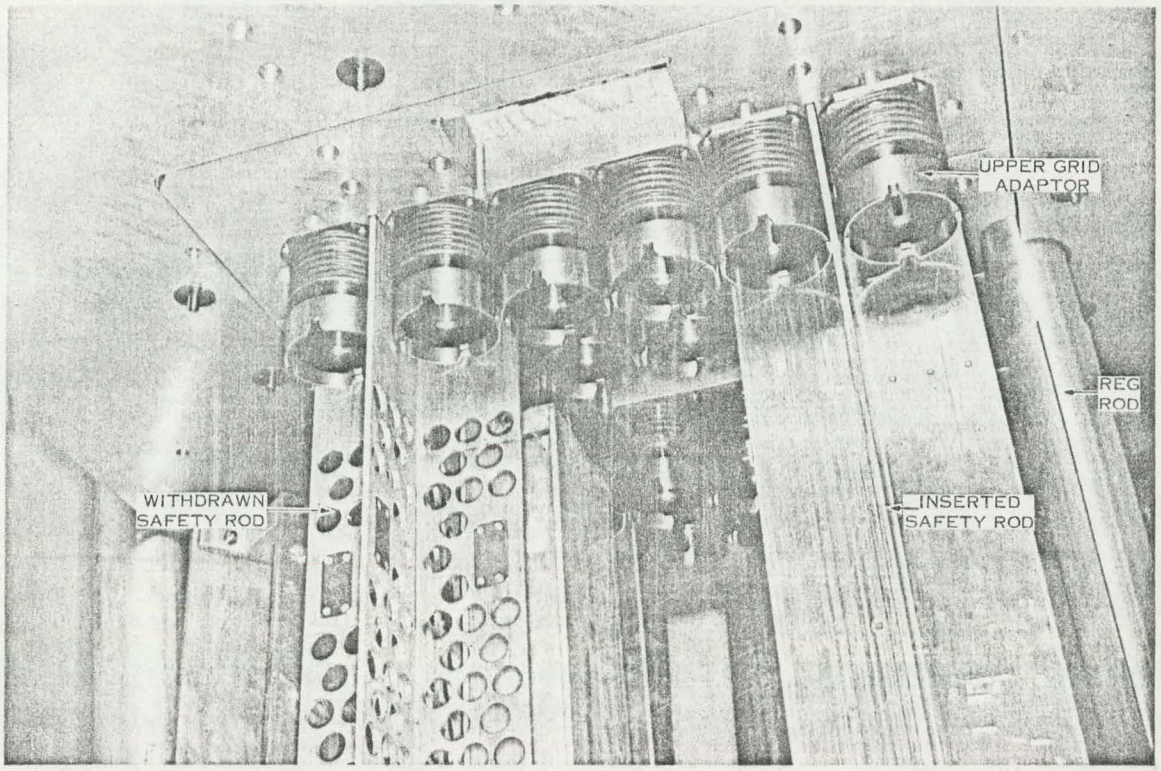

Fig. 8 Bottom view of upper grid.

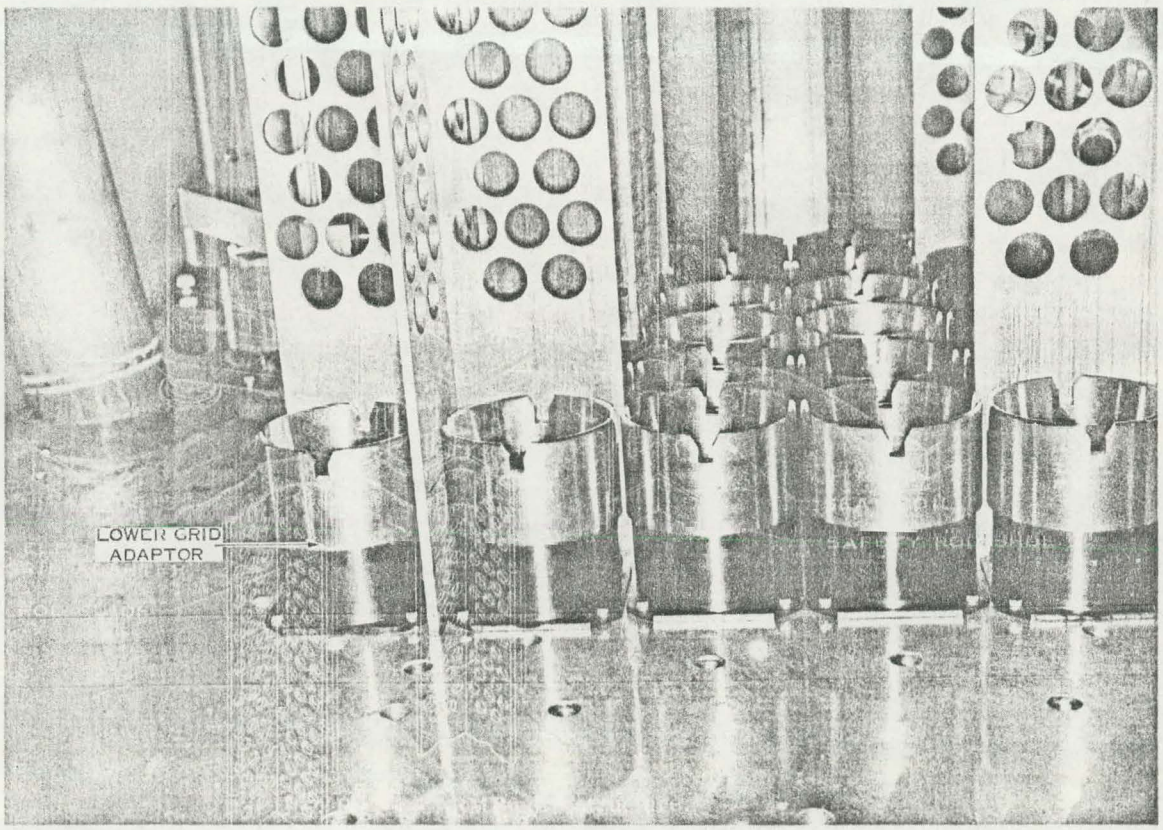

Fig. 9 Top view of lower grid.

2. CORE ARRANGEMENT AND FUEL ELEMENTS

The ARMF core is designed to have three basic features: (a) the ability to determine independently the amount of fuel or poison in a single capsule, (b) a small temperature coefficient of reactivity, and (c) a high degree of symmetry about its midplane and vertical centerline. The ability to determine the amount of fuel or poison in a sample is desirable because some of the ARMF programs call for determination of fuel burnup and fission product buildup after high flux irradiations in the MTR. Separability of the effects of fuels and poisons can be achieved by providing two measuring positions which have markedly different statistical weight ratios of fuel-to-poison. Such a condition is accomplished when one measuring position is near or in the fuel region and the other is far from the fuel region. A small temperature coefficient is desirable to reduce the reactivity drifts caused by canal temperature changes. A high degree of symmetry is desirable because capsules placed at the center of such a core will have minimized scattering effects and theoretical analysis of experiments is simplified. These three design features led to a core design which had a central water-filled volume containing no fuel (flux trap). The results of a study [4] made to determine the core size which would achieve the best compromise between (a) and (b) above indicated that with a predetermined fuel element height of 24 inches, the flux trap should be 6.5-inches-square and the core should be approximately 20-inches-square. Therefore, the fuel elements were made 3.25-inches-square so that the absence of four fuel elements at the center of a 6 x 6 array would produce the desired dimensions.

The fuel elements are of two types, designated Mark I and Mark II. Both are conventional plate-type fuel elements of aluminum, containing fully enriched U-235; both have the same exterior dimensions (Figures 10 and 11). The top and bottom end boxes are identical, in order to provide nuclear symmetry about the horizontal midplane. The end boxes have a chamfer which mates with the countersink in the fuel-element grid-adaptors, previously described. The Mark I element is a plate-type element containing 15 flat fuel plates, pinned to two unfueled side plates. The Mark II element has the same basic construction but is arranged such that it contains a 1.25-inch-square hole at its center. Attached to the tops and bottoms of the fuel plates are capsule holder positioning devices. Mark II elements provide experimental positions with relatively hard neutron spectra.

The physical constants of the fuel loadings are listed in Table I. Based on ARMF-I results, less U-235 was put in ARMF-II Mark I elements as a reactivity shimming measure. Mark II elements for ARMF-1 contain boron so that the elements would give the desired reactivity shimming but, at the same time, possess the same macroscopic absorption cross section as the Mark I element. Any of the elements are physically interchangeable between the two reactors, but to date they have been used only as shown in the table.

Although ARMF-I and -II are structurally identical, the increased interest in resonance integral measurements and thermal absorption measurements has made it advantageous to load ARMF-II with cores which have increased sensitivity to absorption. This has entailed reducing the fuel loading by eliminating the central water hole. Core loadings for ARMF-I and two for ARMF-II are shown in Figures 12, 13, and 14. As can be seen in the figures, all cores have fourfold symmetry about their centers. In ARMF-I, the four safety rods and Mark II elements are symmetrically located, and only the shim and regulating rod

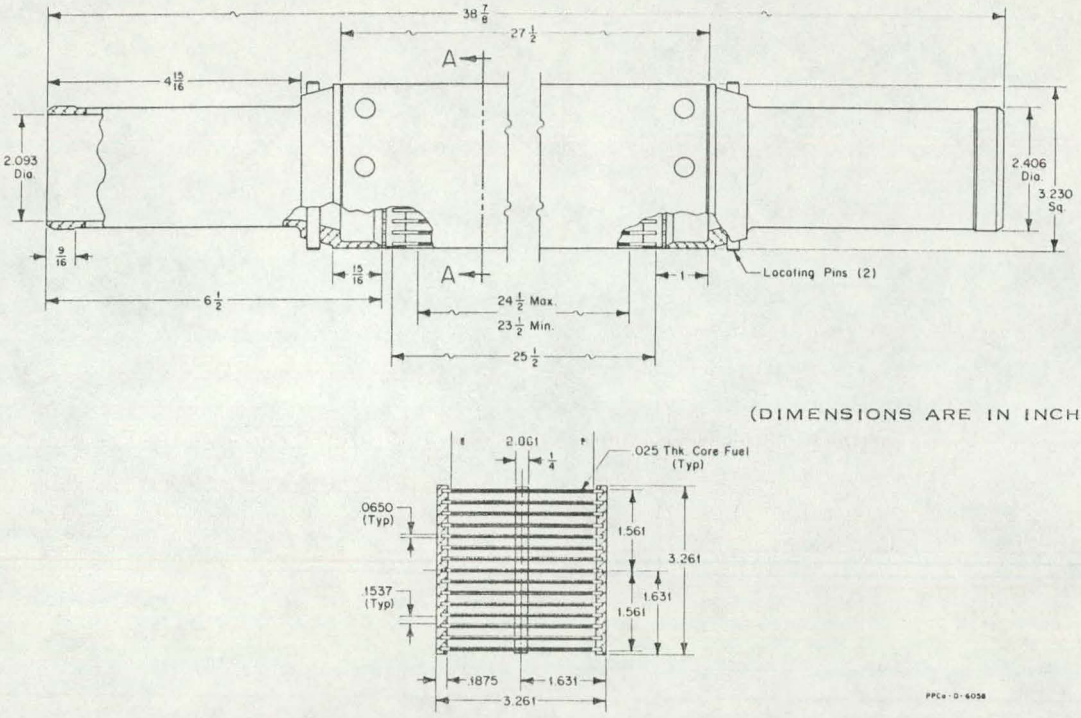

Fig. 10 ARMF Mark I fuel element.

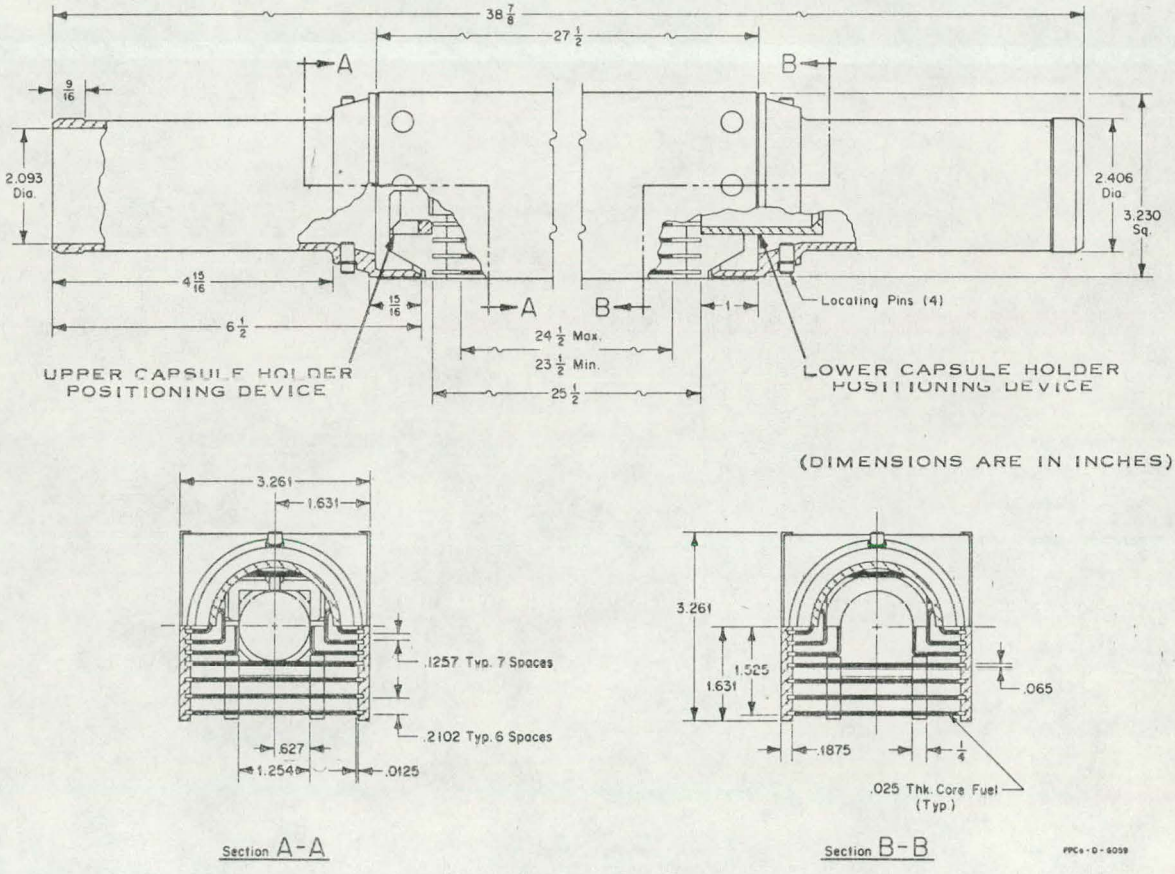

Fig. 11 ARMF Mark II fuel element.

TABLE I

PHYSICAL CONSTANTS FOR ARMF FUEL ELEMENT LOADINGS[a]

	ARMF-I		ARMF-II	
	Mark I	Mark II	Mark I	Mark II
Element Total Volume	4207.99 cm^3	[b]3583.60 cm^3	4207.99 cm^3	[b]3583.60 cm^3
Total Metal Volume	1572.15	[b]1333.43	1572.15	[b]1333.43
Total Water Volume	2635.84	[b]2249.30	2635.84	[b]2249.30
Metal-Water Ratio	0.5965	[b]0.5930	0.5965	[b]0.5930
U-235[c]/Element	188.5 g	150.6 g	179.0 g	130.8 g
Natural Boron/Element	0.0	0.78 g	0.0	0.0
Σ_a(235)	0.0771 cm^{-1}	0.0723 cm^{-1}	0.0732 cm^{-1}	0.0628 cm^{-1}
Σ_a(238)	0.00005	0.00005	0.00005	0.00005
Σ_a(Boron)	0.0	0.0078	0.0	0.0
Σ_a(Al)	0.0052	0.0052	0.0052	0.0052
Σ_a(H_2O)	0.0138	0.0139	0.0138	0.0139
Σ_a(Total)	0.0961	0.0992	0.0922	0.0819
Σ(Fission)	0.0654	0.0613	0.0621	0.0533

[a] All cross sections are based on 2200 m/sec microscopic cross sections.

[b] Water in the center hole is not included except for a 0.01 in. film next to fuel plates.

[c] 93% enriched.

disturb this symmetry. These rods cause reactivity perturbations of only 0.3 and 0.12 percent, respectively. Because the core could not be centered among the safety rods, the ARMF-II loadings are slightly less symmetrical. This produces a very small effect, however, since a withdrawn safety rod has a small perturbation (Section III-3). The compact loadings used in ARMF-II require a shim extension as shown in Figures 13 and 14. The alternation in the orientation of the fuel elements is to prevent the sideplates of adjacent elements from being juxtaposed. During initial operation, when the core was not loaded in this manner, crevice corrosion resulted because the water channel width between the juxtaposed sideplates was only 0.02 inch which inhibited water circulation.

3. SAFETY RODS AND DRIVES

The cruciform safety rods (Figure 7) were each milled from a single aluminum billet. Each of the rod's four blades is 0.25 inch thick. In the upper part of the rod, each blade has a milled recess on one side to accommodate a cadmium sheet, 0.04 inch thick by 3 inches wide by 26 inches long. The cadmium is held in place by an aluminum cover plate riveted through the cadmium to the

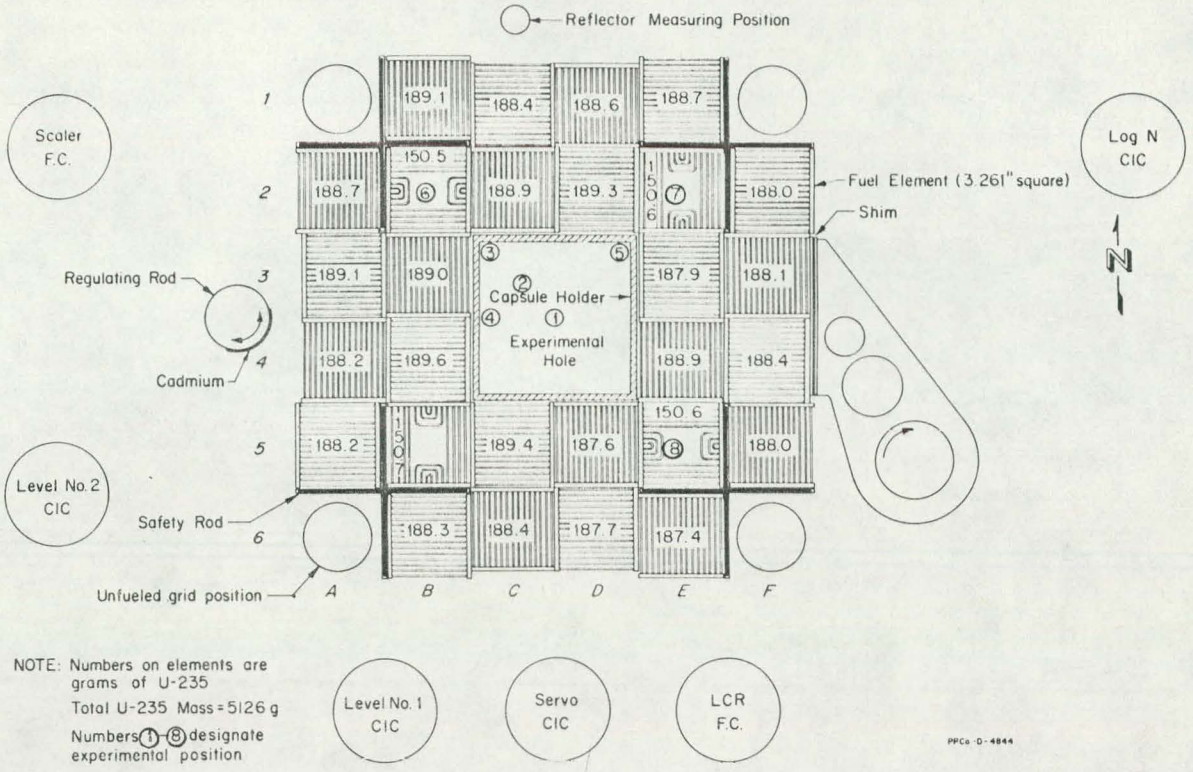

Fig. 12 ARMF-I core loading (2-62).

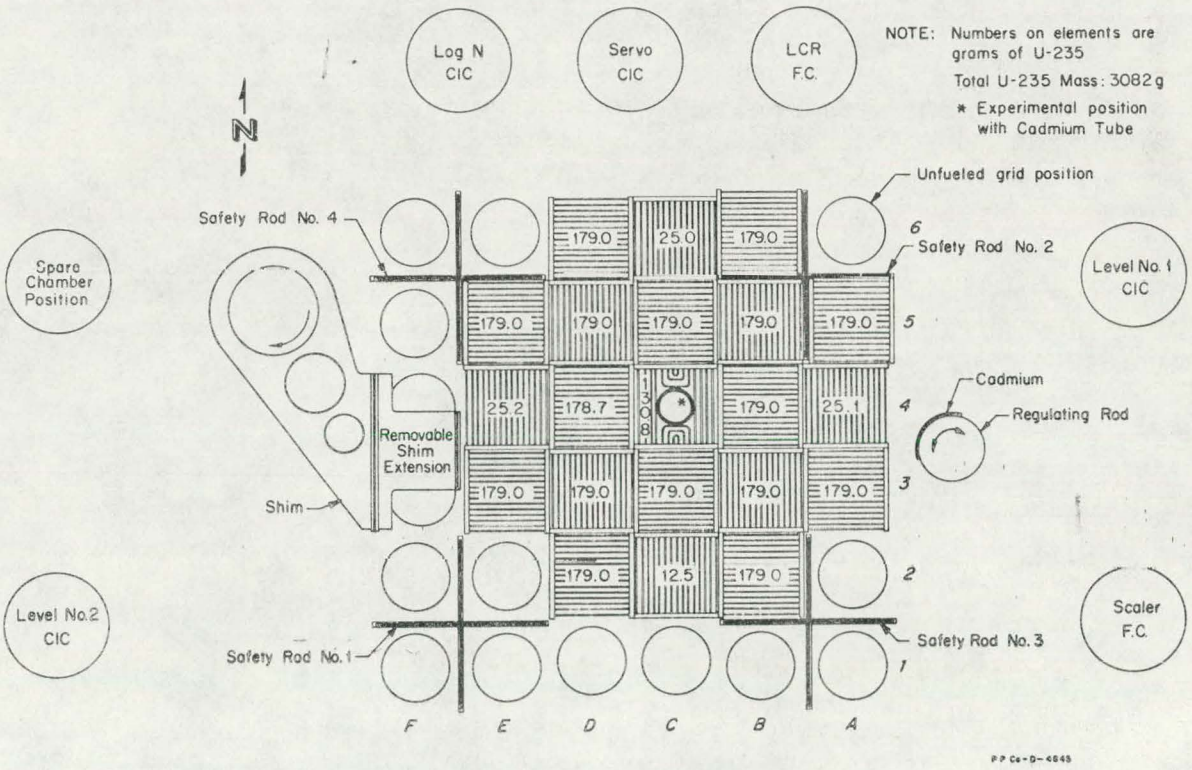

Fig. 13 ARMF-II core loading (4-63).

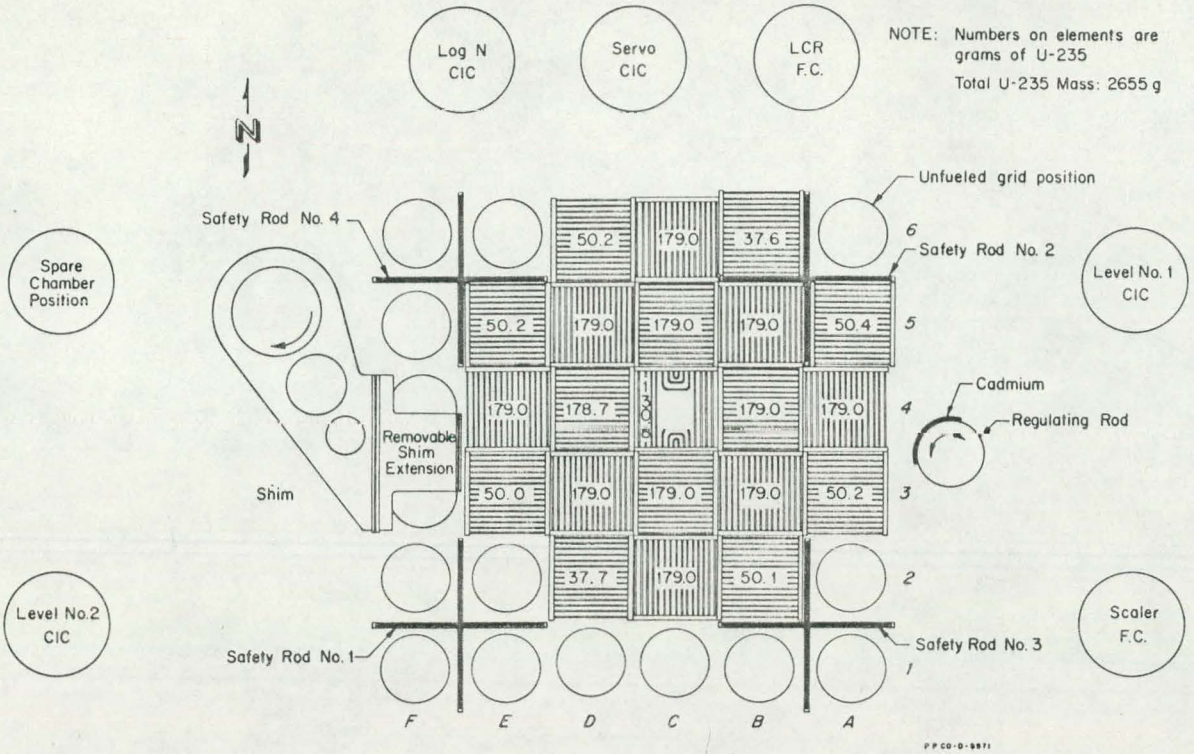

Fig. 14 ARMF-II core loading (3-64).

rod, and an epoxy sealer protects the cadmium from the water. The lower part of the rod, or follower, is perforated so that the core space provided for the safety rod will have the same metal-water ratio as the average of that in a fuel element grid cell. The rod is designed for a withdrawal of 30 inches (compared to the 24-inch fuel plates) which places the bottom edge of the cadmium 5 inches above the top edge of the fuel when the rods are withdrawn to their upper limit. With this arrangement, the safety rods produce a negligible perturbation at the top of the core. This is desirable for two reasons: the vertical flux distribution is not perturbed, and any positioning variations due to the upper limit switch have very small reactivity effects.

The safety rod drives (Figure 15) incorporate a ball-nut screw arrangement for driving the safety rods. The screw, rather than the ball-nut, is driven so that the drive does not extend above the core as would be required with a rack and pinion. This arrangement permits a lower elevation of the working platform deck. The screw is driven through a gear train by a three-phase, 220-volt, one-quarter horse-power, synchronous speed motor. In order to avoid any uncertainty in the direction of rod travel, a monitoring circuit will scram the reactor if one phase of the three-phase power is lost. The rod positions are transmitted to the control console by a pair of selsyns; the one at the console drives a veeder-root counter which displays the position with a resolution of $\pm$ 0.01 inch.

The safety rods are coupled to their drives through electromagnets (Figure 16) which release the rods within approximately 15 msec upon receiving an electronic scram signal. The rods fall into the core under the force of gravity and with an initial acceleration of approximately 0.6 g.

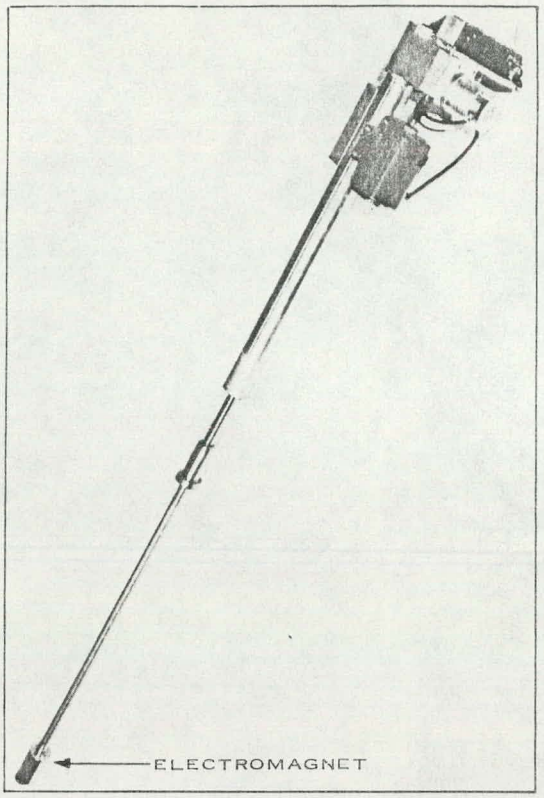

Fig. 15 ARMF safety rod drive.

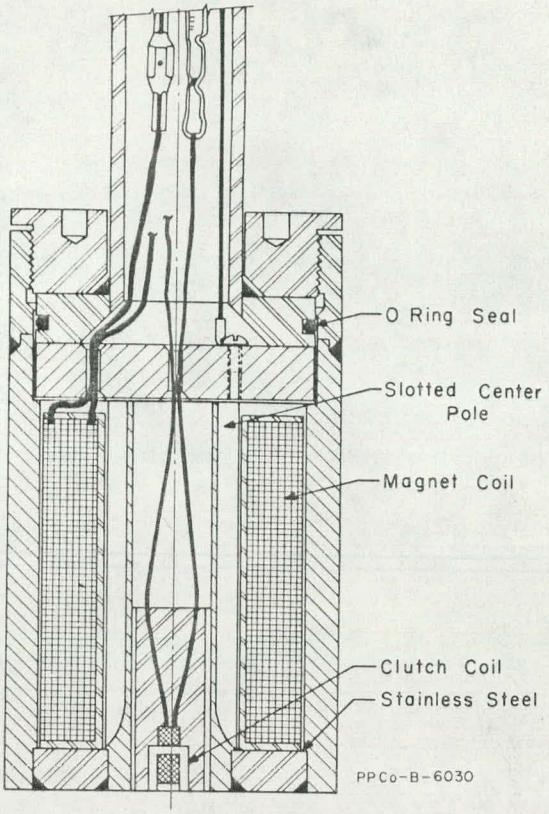

Fig. 16 ARMF safety rod drive electromagnet.

The mechanical shock imparted to the core by the safety rods has been minimized by (a) limiting contact of the rods with the core lattice to two guide rollers per rod on each grid (Figure 7), and (b) mounting the safety-rod shock absorber, a foam plastic pad, on the canal floor rather than on the reactor structure (Figure 6).

4. SHIM ROD AND DRIVE

The shim rod which provides coarse reactivity shimming is located outside the core to minimize the flux distortion on the central water hole (Figures 12, 13, 14). To prevent a distortion of the vertical flux distribution, the rod is rotated in a horizontal direction rather than moved in a vertical direction. The poisoning in the shim is a sheet of cadmium, 0.04 inch thick by 6 inches wide by 24 inches high, sandwiched between riveted aluminum sheets and protected from the water by a coating of epoxy sealer. This assembly is attached with brackets to a "drive" tube (Figure 7) which has a lower bearing mounted on the lower grid and an upper bearing mounted on the control bridge. Mounted on the opposite side of the drive tube from the cadmium bearing plate is a counter balance (not shown in the figures) which minimizes the side load on the bearings.

The rod is driven by a Slo-Syn stepping motor through worm and sector gears. To prevent backlash, the gears are loaded by means of a constant-load

spring motor attached directly to the drive tube. The drive motor is driven with a blocking oscillator, at a rate made variable by the operator, which produces maximum and minimum shim speeds of 6.75 and 0.675 degrees per minute. The shim can also be jogged in steps of one milli-degree by triggering the oscillator through one cycle.

5. REGULATING ROD AND DRIVE

The ARMF regulating rod, located outside the core (Figures 12, 13, and 14), consists basically of a sheet of cadmium mounted on the surface of an aluminum cylinder. The rod (cylinder) rotates about its axis over a range of 160 degrees, thus moving the cadmium toward or away from the core. The cadmium on the regulating rod is a piece 0.04 inch thick by 24 inches high which covers a 126-degree sector of the rod. In both reactors, the cadmium was originally applied by metal spray techniques and was protected from corrosion by a coating of metal-sprayed aluminum. However, the aluminum cladding cracked and blistered after three years operation in ARMF-I; therefore, the cadmium and its aluminum cladding were replaced with sheet material. The cadmium was set in a milled recess in the aluminum cylinder and was covered with an aluminum sleeve which is welded around its ends to the aluminum cylinder. The original cladding, installed in December 1962, is still in ARMF-II.

The regulating rod, with its drive and position transducer arrangement, is shown in Figure 17. The drive motor, tachometer (described in Section IV-3), and position encoder (described in Section IV-2) are coupled directly to the rod (without speed reduction gears) to avoid backlash. In order to minimize alignment problems and make the rod as free running as possible, the regulating rod has only two bearings. The upper bearing is a high precision, self-aligning bearing while the bottom bearing is of a special design. The balls and both races of the lower bearing are made of tungsten-carbide to prevent corrosion and to minimize wear. The inner race is conically shaped to provide accurate self-centering but at the same time allow the

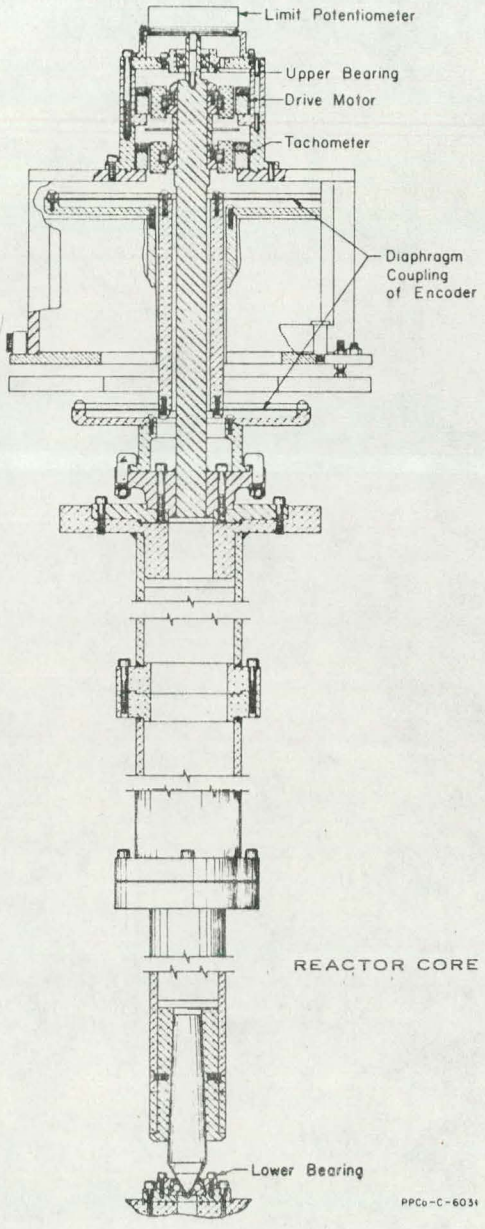

Fig. 17 ARMF regulating rod and rod drive.

rod to be removed without draining the canal. Some difficulty, which is discussed in Appendix B, was experienced with this bearing. The diaphragm coupling of the encoder also minimizes alignment problems, allows for regulating rod expansion or contraction, and avoids the possibility of overloading the encoder if misalignment occurs.

IV. INSTRUMENTATION

The ARMF instrumentation consists of start-up and safety channels, shim and regulating rod position electronics, regulating rod servo control, and auxiliary instrumentation. Commerically available Oak Ridge type instruments are used in the start-up and safety channels, whereas, most of the other instruments were designed and built by Phillip's Instrument Development Branch. The instruments are contained in a console made of relay racks and are arranged as shown in Figure 18. The consoles for both reactors have almost the same appearance except for being a mirror image of one another (Figure 2).

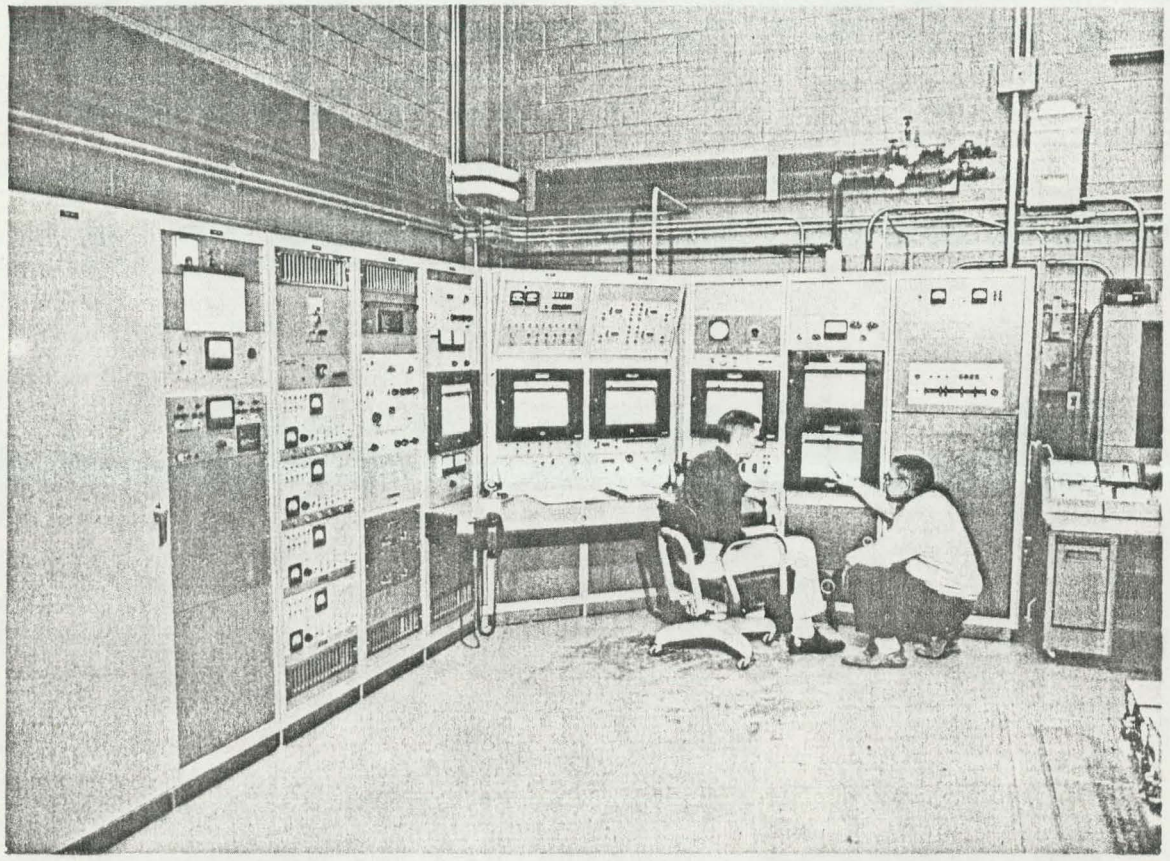

Fig. 18 ARMF control console.

1. START-UP AND SAFETY INSTRUMENTATION

The start-up and safety instrumentation system consists of two start-up channels, two linear level safety channels, and one log N period safety channel, as shown in the block diagram of Figure 19. The safety actions of the control system are listed in Table II. All of the instruments in the start-up and safety channels, except for the sigma preamplifiers, are Oak Ridge designed instruments which are adequately described in the literature [5, 6].

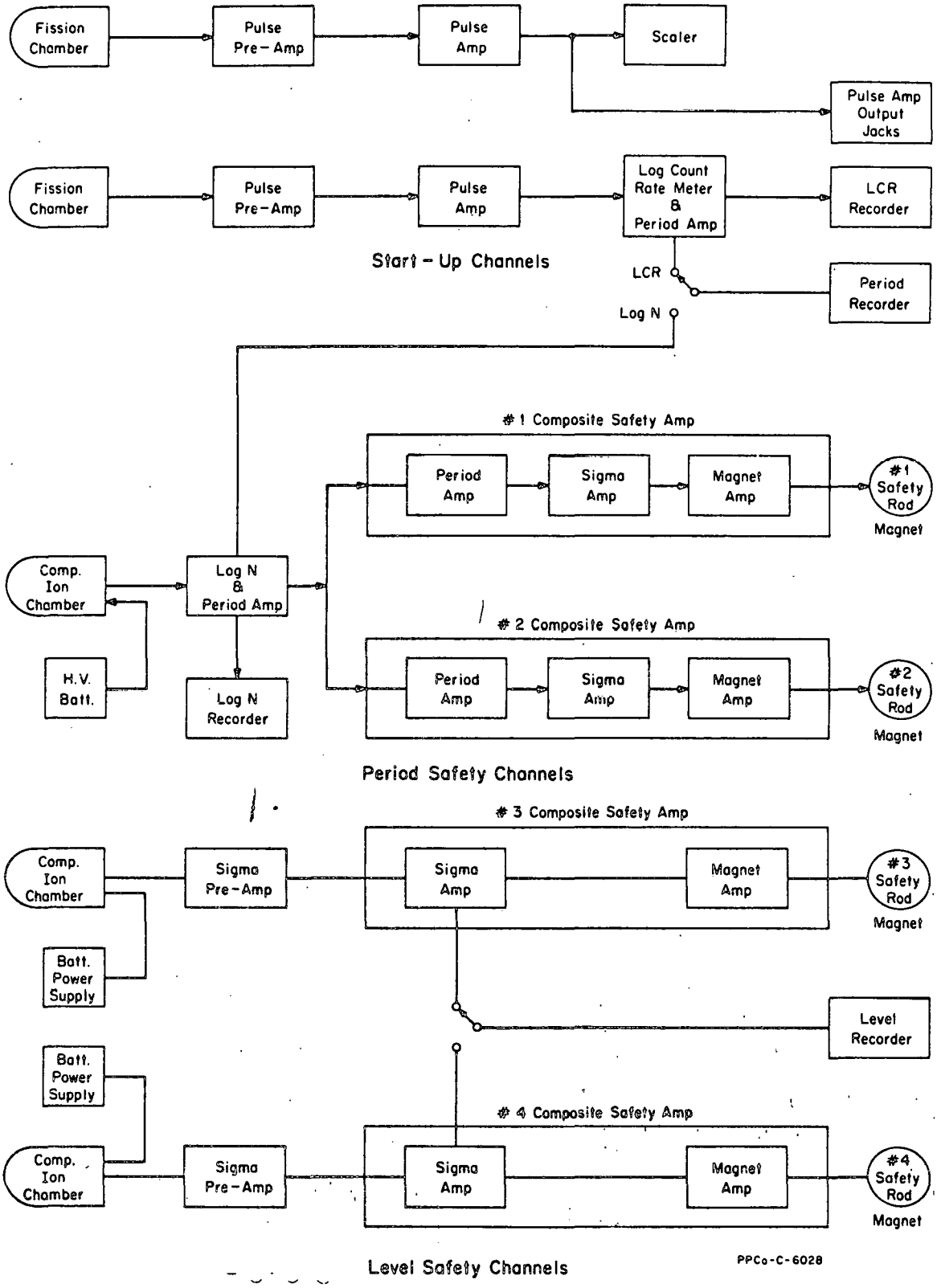

Fig. 19 ARMF start-up and safety instrumentation.

TABLE II

ARMF SAFETY ACTIONS

Instrument	Set Point	Safety Rod Motion
CSA #1	$T \leq 7$ sec	Reverse
	$T \leq 5$ sec	Fast Scram
CSA #2	$T \leq 7$ sec	Reverse
	$T \leq 5$ sec	Fast Scram
Period recorder	$T \leq 20$ sec	Interrupts all rod withdrawals
	$T \leq 15$ sec	Reverse
CSA #3	1300 W	Reverse
	1500 W	Fast Scram
CSA #4	1300 W	Reverse
	1500 W	Fast Scram
Power level recorder	1500 W	Slow Scram

Interlocks	Safety Rod Motion
Regulating rod in LL and AUTO, and shim out of LL	Reverse
Regulating rod in LL and AUTO, and shim in LL	Slow Scram
Manual scram switches on console, bridge, building doors, and switch on overhead crane (crane over reactor) depressed	Slow Scram
Log CR recorder in UL, and Log N recorder in LL	Slow Scram
More than one rod scrammed	Slow Scram
Regulating rod in AUTO, and regulating rod not in UL	Prohibits safety rod withdrawal
Shim not in LL	Prohibits safety rod withdrawal
Log CR recorder in LL	Prohibits safety rod withdrawal
Safety rods not in UL	Prohibits shim withdrawal

Terminology

LL-lower limit, UL-upper limit, AUTO-servo control.

Fission chambers are used in the start-up channels, and compensated ionization chambers (CIC) are used in the other channels because of their capabilities of discriminating against gamma-induced pulses and currents. Gamma discrimination is important because the highly radioactive capsules, frequently measured, produce gamma fields greater than those produced by the reactor core at the chamber locations (≈ 300 r/hr at the nearest chamber for 50 watts of core power). The fission chambers are Westinghouse, Type WL 6377. The location of the chambers is shown in Figures 12 and 13.

The Phillips-designed sigma preamplifier (Figure 19), which replaces the preamplifier in the composite safety amplifier, increases the sensitivity of the channel by a factor of 600. The unit has an automatic gain reduction of ten which (a) extends the on-scale range of the channel, and (b) lowers the scram level from 1500 watts to 150 watts for fast reactor periods. The gain reduction is accomplished by a microswitch in the log N recorder and a 2.5-sec-delay relay. The recorder microswitch is set to actuate when the signal level with the preamp on high gain reaches 100 percent of full power (100 watts). If the reactor is on a period of less than 7 sec, the voltage in the sigma amplifier will reach scram level (150 percent full power) before the 2.5-sec-delay relay reduces the gain. Thus, for fast reactor periods, the scram level is a decade lower than it would be without this feature.

2. REGULATING ROD AND SHIM POSITION INSTRUMENTATION

Accurate determination of regulating rod and shim positions (orientation) in the ARMF is very important because reactivity effects are determined from changes in these rod positions when capsules are inserted in the reactor. Therefore, the rod position instrumentation was designed to give positions as accurately as possible.

Position signals for both rods are derived from optical shaft-angle encoders attached directly, without gearing, to the rod drive tubes (Figure 17). The encoders (Wayne-George Co., Model RD17H) are basically composed of a strobe lamp, encoding disc, a collimating slit, and a bank of 17 photo diodes. The encoding disc consists of 17 coaxial rings of alternate opaque segments photographed on the glass substrate.

The rod position instrumentation, shown in the block diagram of Figure 20, is a digital system made up of solid state components [7]. This system displays the rod positions on the console for operator use and also records rod positions on IBM cards for computer data reduction.

The regulating rod position is displayed on four different instruments. Because the regulating rod is constantly moving, its position is sampled continuously at a selectable rate, usually set at 16 samples per second. The digital signal from the encoder is converted to an analog signal and displayed on two panel meters (one on console, one on working platform) with ranges of 0 to 100 percent of rod motion, and on an 11-inch strip chart recorder which has a span of 1/16 of rod motion. The equipment automatically displays the range within which the rod is positioned. An operational pen identifies, in binary code at the edge of the chart, the range being displayed. If the rod position is such that the rod is hunting

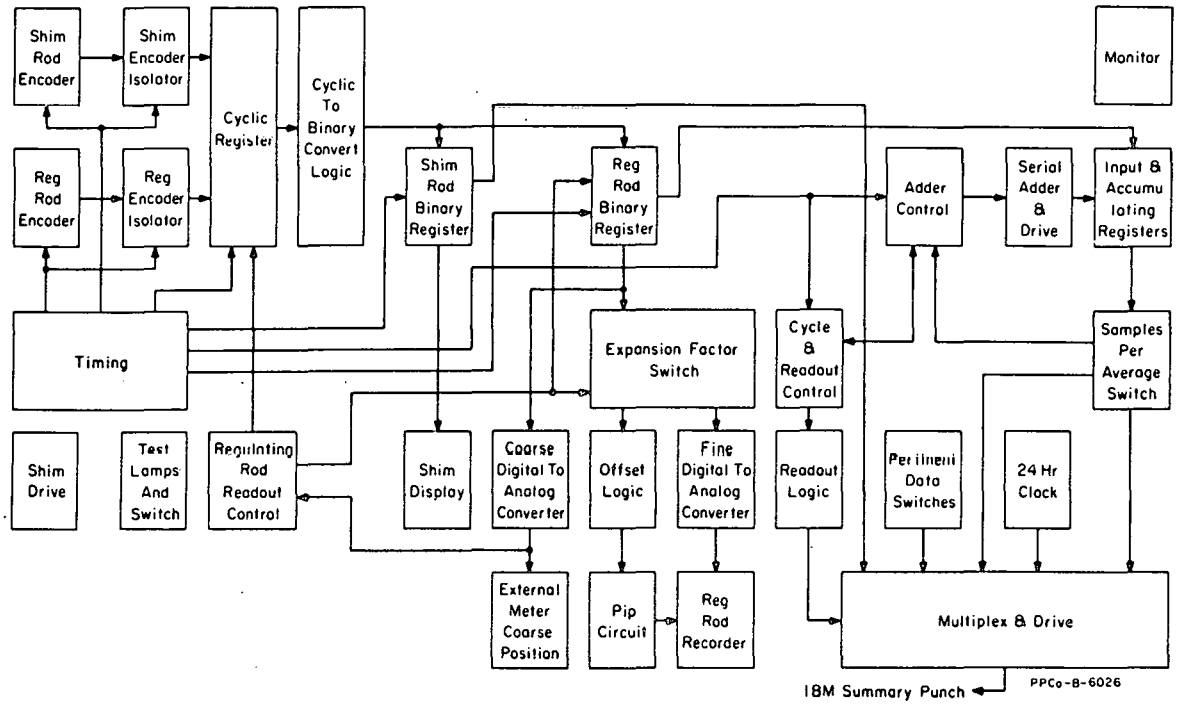

Fig. 20 ARMF regulating rod position instrumentation.

across the boundary of two ranges, an offset of 50 percent of one range is available to the operator. The digital signal is also fed into instrumentation which averages the instantaneous rod positions and punches them into IBM cards. Eight separate rod position averages are accumulated and punched into each card (one card is punched for each capsule measurement) so that reactor stability and drift can be evaluated. The number of rod position samplings that go into each average is determined by the sampling rate and the total sampling time which is selectable from 1/2 to 32 minutes in multiples of two. The number of samples is always a binary multiple so that the average can be calculated by merely displacing the binary point. Each average is punched as six octal digits which give a resolution of 6.4×10^{-4} degrees of arc [a]. This is equivalent to 7×10^{-9} $\Delta k/k$ at the point of maximum differential reactivity worth of a regulating rod, which has a total worth of 1.2×10^{-3} $\Delta k/k$. Along with the eight rod position averages, other pertinent measurement information is recorded on each card: capsule identification, measuring position in reactor, canal temperature, program identification, number of samples per average, time of day, rod position sampling rate, and shim position. The information is scanned from manual entry switches, except for time which is scanned from a digital clock.

The shim position is displayed on both coarse and precise readouts. A coarse position is derived from a selsyn transmitter coupled to the shaft of the drive motor. The selsyn receiver drives a readout register which displays the shim position in decimal form with an accuracy of approximately 5.5×10^{-3} degrees

[a] Resolution this good is needed only for static calibrations because the rod hunts over a range of more than ten times this value.

of arc. An accurate shim position signal is obtained from a shaft-angle encoder. The associated electronics are combined with the regulating rod position electronics as shown in Figure 20. The shim position, in octal code, is displayed on a bank of 14 lamps on the console and is punched into each IBM card as mentioned in the foregoing. The resolution of the digital readout is 2.8×10^{-3} degrees of arc, but the shim can be jogged in 9×10^{-4}-degree steps so that the shim position is known to within $\pm 5 \times 10^{-4}$ degrees. A rotation of 5×10^{-4} degrees causes a reactivity effect of 0.15 μk ($\mu k = 10^{-6} \Delta k/k$) at the point of maximum differential worth (inner limit) and 0.1 μk at typical operating positions.

3. REGULATING ROD SERVO CONTROL SYSTEM

The servo controlled regulating rod is the primary measuring scale of the ARMF. By means of a compensated ionization chamber and the appropriate amplifiers (Figure 21), the regulating rod is controlled at a position which maintains the reactor critical and at a constant and preset power level. The reactivity effect of a capsule is thus obtained from the regulating rod positions before and after capsule insertion and a predetermined regulating rod calibration (Appendix C).

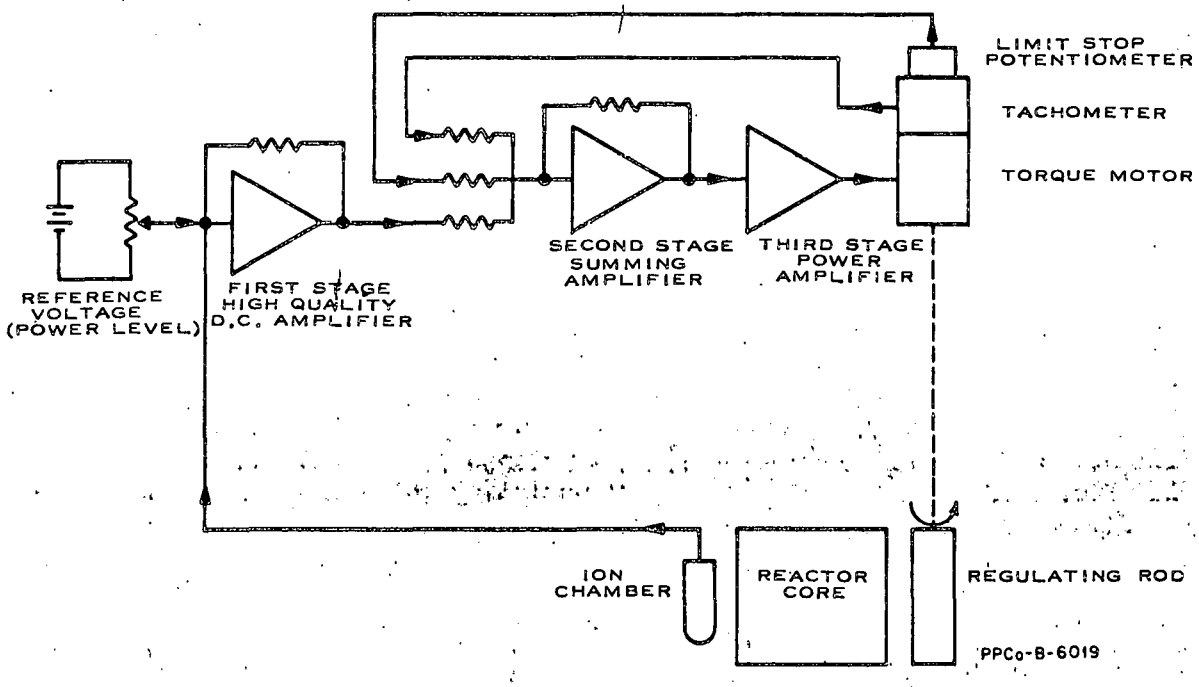

Fig. 21. ARMF regulating rod servo control system.

As can be seen by looking at Figure 21, this regulating rod control system is basically a conventional direct-current servo system. The signal applied to the first stage of amplification is the difference between a current proportional to the power level of the reactor as measured by an ion chamber, and a current obtained from a reference voltage source. This power level error signal is then amplified and used to drive the regulating rod to correct for any power level

deviation. The required amplification between the ion chamber and torque motor is obtained by three amplifier stages of solid state electronics. Three stages are used, partly for the convenience of breaking up the amplification by function and partly to obtain compatible impedance levels. The first stage is a high quality, direct-current amplifier with low drift characteristics. The second stage is used to add in and adjust the gain of the tachometer and limit stop signals. The third stage provides the necessary power amplification to drive the torque motor.

Electrical feedback signals are used to provide the necessary loop stability and a cushioned limit stop. Because it is rugged and has no limit stop, a torque motor, wound for use as a tachometer, is used to provide loop stability. Rather than using conventional limit switches, limit signals are derived from a specially wound potentiometer which gives an output signal only when the desired end-of-travel limit is reached. The tachometer and limit switch arrangement can be seen in Figure 17. The potentiometer, used as a voltage divider, produces a signal which gradually increases as the limit is approached until it becomes equal but of opposite polarity to the servo driving signal. The limit, therefore, stops the rod with a cushioning effect. To avoid any possibility of mechanical shock to the regulating rod system, mechanical stops in the entire regulating rod system were avoided; thus, the rod can rotate freely if a limit signal should fail. This feature does not present a potential hazard since the rod is worth only 0.12 percent $\Delta k/k$.

4. AUXILIARY INSTRUMENTATION

Auxiliary instrumentation, which is either somewhat unusual or quite important to the ARMF purpose, is described in this section. The instruments described are the temperature measurement bridge, safety rod clutch and seat indicators, bypass annunciator and trouble monitor, and radiation monitors.

4.1 Temperature Measurement Bridge

The temperature measurement bridge is a sensitive narrow span instrument capable of detecting and recording canal temperature variations of 0.001° C. This sensitivity is achieved by using a thermistor with a temperature coefficient of resistance of -4 percent/°C in a Wheatstone bridge circuit. The unbalanced condition of the bridge, created by temperature fluctuations, is measured and recorded by a 0 to 500 microvolt, Minneapolis-Honeywell recorder. The temperature span that is permitted with this sensitivity is $\pm$ 0.025°C, but it can be measured about any temperature by balancing the bridge at that temperature. The instrument also has less-sensitive ranges with spans of $\pm$ 0.25 and $\pm$ 2.5°C.

The temperature probe is a bead-in-glass type thermistor sealed with epoxy resin in an aluminum tube. The tube reaches from above the water surface to the reactor core. The probes can be removed for recalibration or replacement in case of breakage.

4.2 Safety Rod Clutch and Seat Indicators

A proximity device is used to supply the operator with information as to whether or not the safety rod is attached to its magnet. This device consists of

two parts: (a) a sensing coil made up of a coil wound on an open "c" core and (b) a transistorized control unit containing a 1 kc oscillator, amplifier, and power supply. The device utilizes the decrease in impedance occurring when the open side of the core comes into proximity with a soft iron armature. The coil is cast in epoxy resin at the center of the safety rod magnets (Figure 16) in ARMF-II, but they are attached to the outside of the magnets in ARMF-I. The proximity unit (or clutch) is, therefore, actuated when the magnet engages (or "clutches") the safety rod.

Information as to whether the safety rods are fully inserted in the reactor core (in their seat) also is derived from a proximity unit identical to the clutch unit. The seat coils are mounted on the underneath side of the lower grid with their faces near the surface of the safety rod (Figure 7). The seat coil armature plate is a small piece of chromium-plated armco iron imbedded in the rod.

4.3 Bypass Annunciator and Trouble Monitor

Several of the control system interlocks must be bypassed to permit instrument calibrations and control system check-out. These interlocks have been provided with bypass switches. To prevent an inadvertent bypass, all bypasses are monitored and annunciated by a pair of flashing lamps and identified by individual lamps.

Those parameters important to the safe and efficient operation of the reactor (eg, signal cable connections, chamber voltages, and calibration switch positions) are also monitored with a trouble monitoring system. If conditions are not as prescribed for operation, the condition is annunciated by a pair of flashing lamps and identified by individual lamps.

4.4 Radiation Monitors

The ARMF building is monitored by two stations of the MTR remote monitoring system (RMS). Each station, consisting of a detector, amplifier, alarm unit, and power supply, covers a six decade range, 0.1 mr/hr to 100 r/hr. Audible and visible alarms are located at each station. Level meters, alarms, and recorders are also located in the MTR Health Physics Office.

The building is also monitored for airborne radioactive particles. This monitor is equipped with a linear automatic-range-change ratemeter (3 ranges), a gas sampler, a pumping system, a detector, and a power supply. Audible and visible alarms are located on the instrument.

To warn the operator of inadvertent removal or radioactive capsules from the water, a gamma sensitive radiation monitor is located just above the surface of the water on each reactor structure. The instrument is typically set to alarm at 10 mr/hr.

V. EXPERIMENTAL EQUIPMENT

The experimental equipment consists of (a) capsules of various types containing the material (sample) to be measured, (b) an overall framework (capsule holder) for positioning these capsules in the reactor, and (c) tools for movement of the capsules or other equipment. The exact and reproducible positioning of any capsule is of utmost importance in getting precise reactivity measurements. Qualitatively, the effect will be least where flux and adjoint gradients are a minimum, ie, in the positions of greatest core symmetry. Capsules and capsule holders are designed to give as precise positioning as possible, consistent with ready movement of the capsules.

1. CAPSULES

A wide variety of capsules has been used in ARMF measurements. Capsule design, in general, is a compromise among the factors of program purpose, capsule size, sample material, handling convenience, and the statistical weight of the experimental position (usually, however, capsules are designed to be measured in any experimental position). As mentioned in the foregoing, one of the most important considerations is the capability of precisely positioning the capsule in the ARMF; however, program purpose may force a compromise in this feature. For example, if a capsule is to be irradiated in the MTR or ETR, the design must include heat removal features which may not be compatible with precise positioning features; moreover, the capsule may "grow" during irradiation or become deformed (burred, etc) through handling, which also presents a positioning problem. Examples of capsule designs which are a result of these considerations and problems are shown on a one-inch grid in Figure 22 and are discussed below.

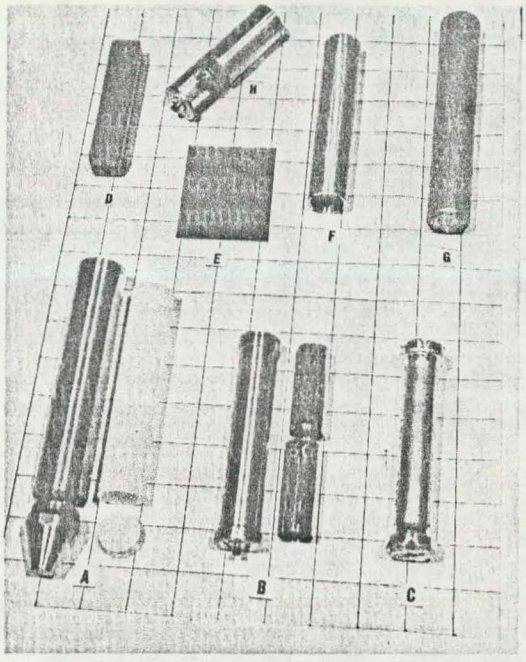

Fig. 22 Examples of capsules used in ARMF programs.

Type A is an example of a capsule of which the major design feature is precise positioning. It consists of an aluminum outer capsule and a close fitting polyethylene inner capsule which is commonly used for liquid samples. So that a change in orientation does not displace the capsule contents, the wall thickness of both capsules is held to very close tolerances. The outer capsule is as large as practicable for use in the Mark II fuel element experimental hole, and its empty weight is greater than its buoyancy. Its cap (bottom end) has a 40 degree included-angle taper which, when placed in a matched

socket in the capsule holders, has given very accurate positioning [a]. Both capsules have threaded caps; the outer capsule is sealed with an O-ring, whereas the inner capsule can be sealed with heat if a positive seal is necessary.

The type B capsules are of aluminum and designed for use in the air tube (Section V-2). The capsules are thin-walled tubes with an end cap that screws on to retain the hollow cylindrical sample sleeves which are also shown.

Type C capsules are used for burnup and fission product transient studies of fuel samples irradiated in the MTR or ETR. The thin-walled, hollow cylindrical body is designed for maximum heat transfer during irradiation. The end caps direct water flow through the center. Two separate small diameter tubes inside the capsule contain flux monitor wires for nvt measurements during irradiation. These capsules are loaded into aluminum baskets, similar in design to the type A capsule, for positioning in the ARMF.

Type D capsules consist of a cluster of four rods, 3/8 inch diameter and 4 inch long. Each rod contains 8-3/8-inch-square cylindrical pellets of sintered UO_2. The rods, fuel, and spacing are typical of the PWR blanket. These capsules have been used to study the reactivity effects of long term irradiation.

Several other types shown include: E -- the flat plate of the Fuel Plate Development Program; F -- a thin-walled zirconium clad thorium capsule for long term irradiation studies; G -- a solid cylindrical thorium slug; and H -- a capsule similar to type B, for powdered samples.

2. CAPSULE HOLDERS

Capsule holders are used to position capsules accurately and reproducibly in the ARMF during a reactivity measurement. They are, in general, of three types: (a) the universal holder designed for the central experimental hole of ARMF-I; (b) inserts for the Mark II fuel element; and (c) the air-filled tube (air tube). The first two can be adapted to take any type capsule, whereas the last is for capsules of types B and H (Figure 22).

The universal holder is shown in Figure 23 and in the cutaway view of the reactor core, Figure 7. It is a square frame of 1/4-inch-thick aluminum plate with most of the material removed at the center. The lower end is supported and positioned by a matching taper and chamfer, while the upper end is positioned by two steel pins. Sets of lucite or aluminum, guide and positioning plates are mounted in this framework. The plates are tailored to the needs of individual capsules to give the desired position, both vertically and horizontally. A series

[a] Originally the cap was made with a 90 degree, included-angle taper and was positioned by two plates or as in the Mark II element, by a side supporting holder. The bottom of the capsule was positioned by a plate containing a matching chamfered socket, but the top was positioned by a second plate containing a hole large enough to pass the capsule. To provide adequate clearance, the hole had to have a 0.005 inch larger diameter than the capsule. Thus, a variation of 5 mils was allowed in the position of the capsule top. The new positioning method has eliminated the need for the upper plate except as a guide to the bottom socket. The new method has also simplified Mark II element holder designs.

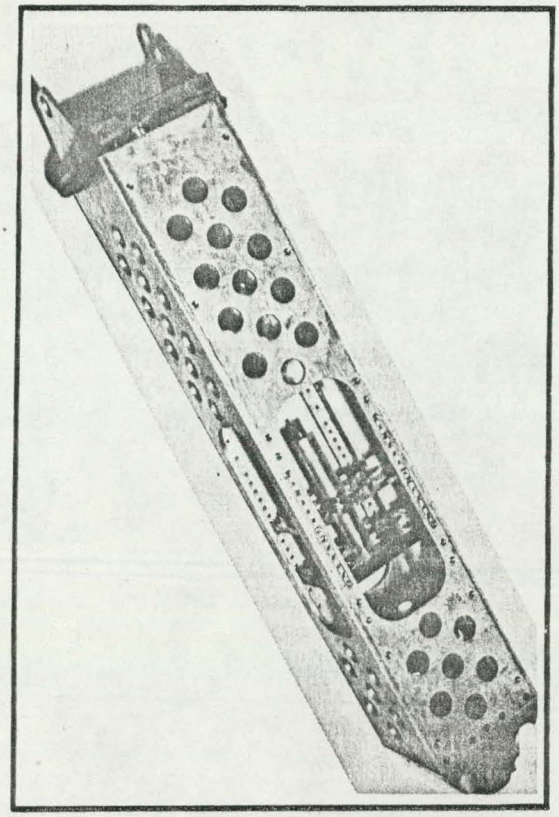

Fig. 23 ARMF universal capsule holder.

of closely-spaced holes in the holder frame allows a selection of vertical positions.

One type of capsule holder for a Mark II element is shown in Figure 24. The lower item clamps to the lower end of the fuel element where it remains, unless some special requirement dictates its removal. (Removal can be accomplished remotely with a special tool.) It has a 40-degree, chamfered socket for positioning the spacer piece (center piece in the figure). The spacer piece has the upper end machined to accommodate the capsule type being measured and is made long enough to center the capsule in the core. The one illustrated is for use with capsules of type A. Miscellaneous other holder types are used for capsules which cannot be positioned in the same way as the type A. Some of these holders extend the full length of the fuel plates and are positioned by the Mark II element positioning devices at the top and bottom of the fuel plates (Figure 11).

The Mark II elements and the central experimental hole have been designed to accommodate a facility which would extend through and below the lower grid (eg, capsule oscillator).

In addition to these holders, an air-filled tube (air tube) facility is available for the measurement of capsules in the absence of water (eg, resonance integral measurement). An assembly sketch of the tube and capsule holder is shown in Figure 25. The major portion of its length is a 2-inch-diameter, aluminum tube extending from just above the core to above the water surface. The lower portion, of about 1.25-inch OD, extends into and through the core and is attached to the upper tube by a flange containing an O-ring seal. This replaceable lower extension is a thin-walled, aluminum tube with or without a 6-inch cadmium shielded volume at its midsection. The cadmium shield is used specifically for resonance integral measurements. Type B capsules are attached to a plastic and aluminum capsule holder which contains a cadmium lid when needed for the cadmium shielded volume. The capsule holder also contains a seat indicator consisting of batteries, light, and switch. Handling of the capsule holder is done with a steel, oil-tank gauging tape.

3. HANDLING TOOLS

A variety of tools has been designed to handle the capsules, both in and out of the ARMF; representative ones are pictured in Figure 26. When conveniently possible, the capsules are attached to a nylon fishline with a fishing reel.

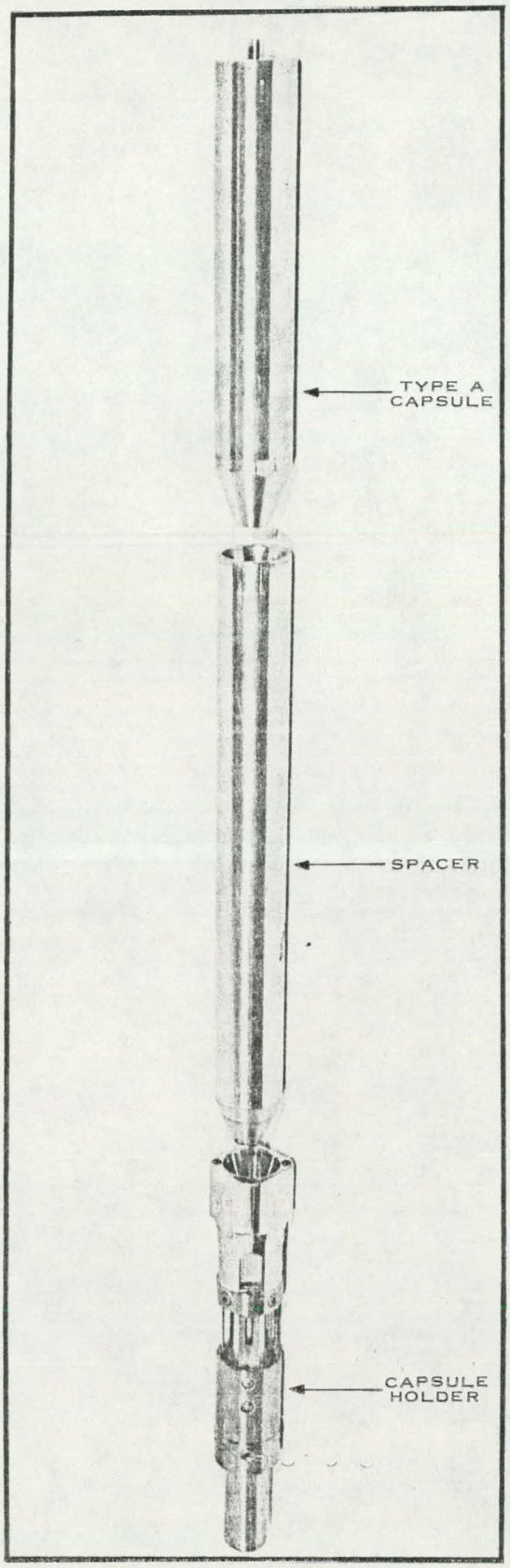

Fig. 24 ARMF Mark II fuel element capsule holder, spacer, and type A capsule.

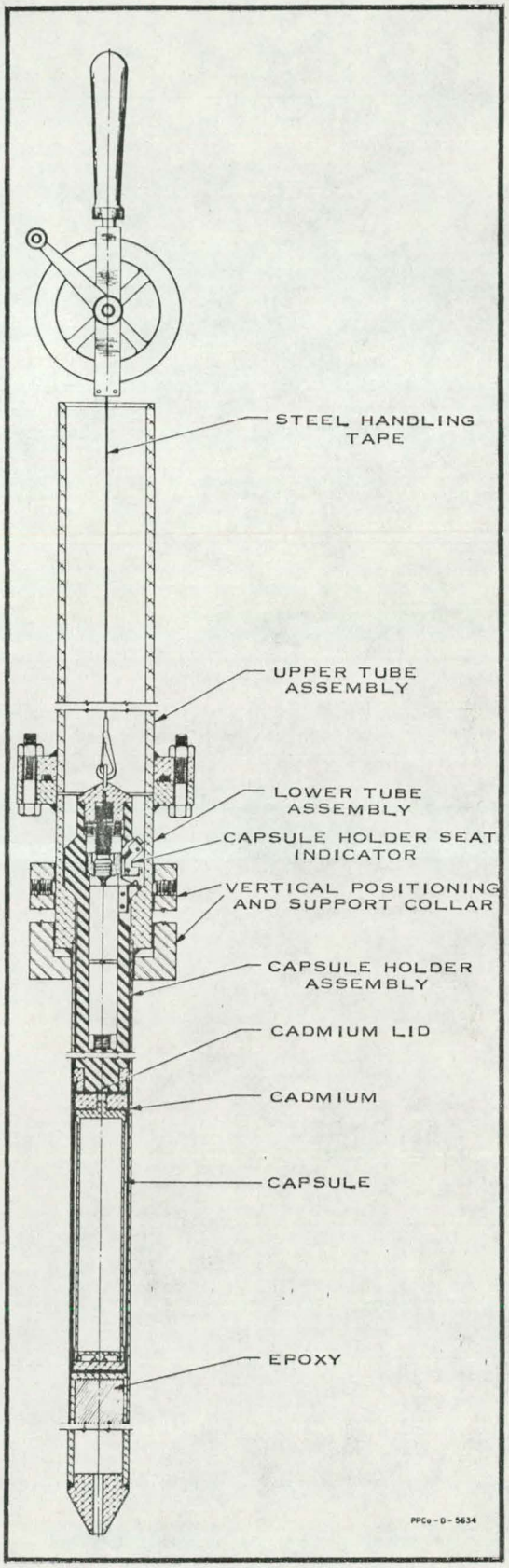

Fig. 25 ARMF air tube and capsule holder.

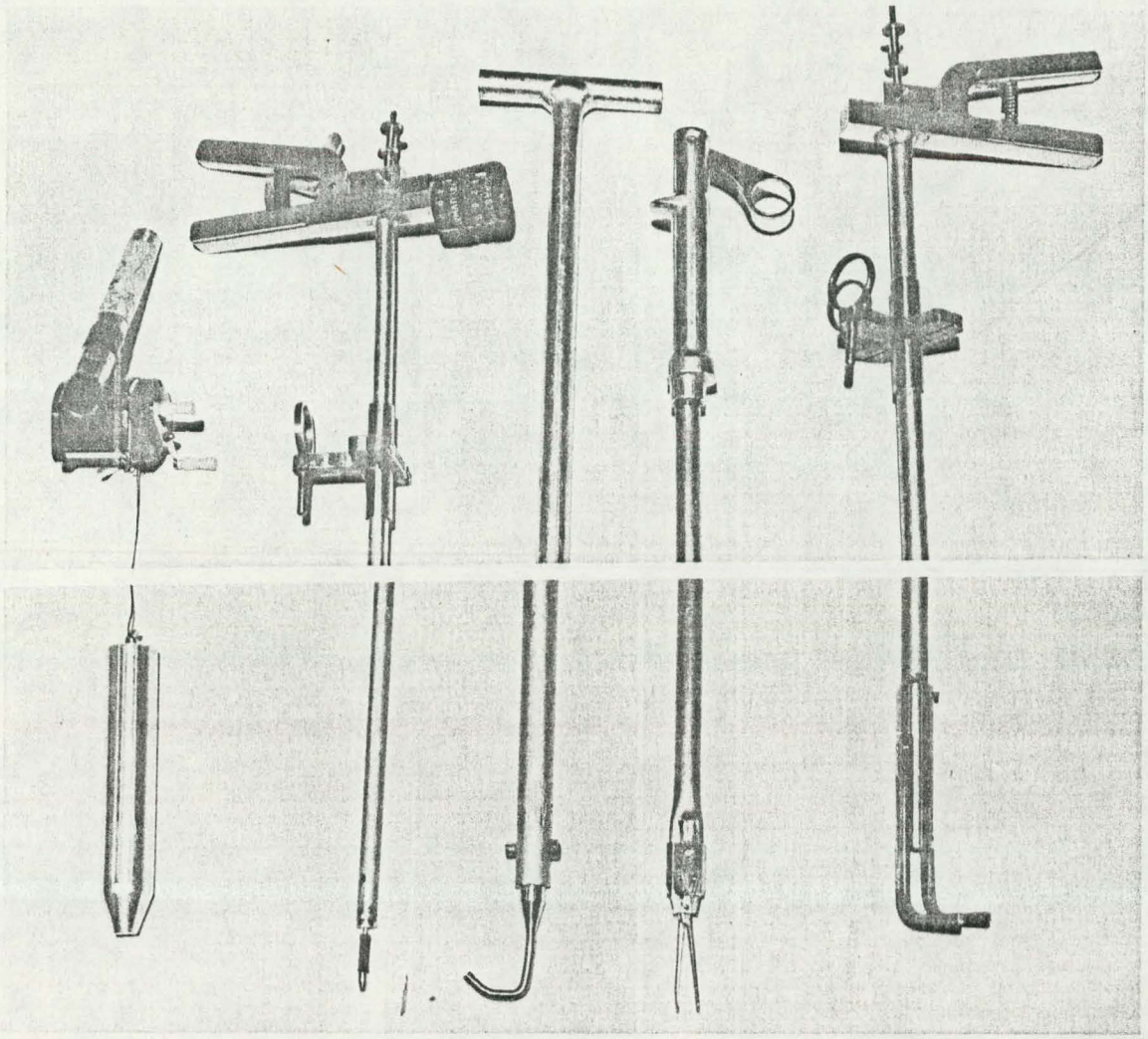

Fig. 26 ARMF capsule handling tools.

In the case of irradiated capsules, a metal disc is tied into the line to prevent inadvertently reeling the capsule too near the surface of the canal and thus causing excessive radiation exposure of personnel.

The rigid rod type tools are generally made with 3/4-inch hollow aluminum tubing for light weight. Most of the tools are approximately 16 feet long. These consist of both the clamping type for slugs or plates and an expansion type. The latter tool, shown second from the left in Figure 26, was designed by Westinghouse for use in their ARMF programs. When actuated, it causes the rubber tube near its tip to be compressed longitudinally, thus expanding it slightly in the lateral dimension. Any capsule with a center hole near the diameter of the original rubber tube can be readily handled in this way. For handling capsule holders or fuel elements, hook tools and various wrench tools, designed for specific application, are also available.

VI. NUCLEAR CHARACTERISTICS

1. NEUTRON FLUX DISTRIBUTIONS

Thermal neutron flux distributions and spectral information in a reactor are necessary in planning experiments and interpreting results. The information from experimental positions is of primary importance. The data given below are selected from typical situations or positions, with emphasis on those of direct application to capsule measurements. Results are presented principally as graphs of thermal flux and of F_1, the spectral index introduced by Nisle[8]. The relationship between F_1 and the equivalent cadmium ratio for a 1/v absorber or between F_1 and Westcott's "r" factor[9] is also given in Reference 8.

All neutron flux data presented have been normalized to a reactor power of 30 watts.

1.1 Core Neutron Flux Distribution

Vertical distributions of thermal flux in fuel elements are of the usual cosine variation, with the maximum at the center of the element. As typical, the data from Element D-5, ARMF-I, are plotted in Figure 27. The increase in thermal flux in the water reflector, observed at the top and bottom, is normal and due to the sudden change in neutron absorption.

Typical of the spectral variation is the plot of F_1 as a function of vertical position for element D-4, ARMF-II, as given in Figure 28. The value of F_1 remains reasonably constant over most of the core height.

Figure 29 shows two traverses at the horizontal midplane along the east-west centerline of ARMF-I. When the shim was withdrawn to 10.3 degrees (no capsule in reactor), excellent flux symmetry exists, with only a small perturbation near the shim (east side); however, this perturbation becomes more pronounced when the shim was moved to 3.9 degrees to compensate for the fueled capsule at the center. A pronounced effect on the flux pattern also exists in the central experimental hole.

A north-south horizontal traverse through the center of the F fuel row, ARMF-I, is shown in Figure 30.

1.2 Experimental Hole Neutron Flux Distribution

A contour map of the thermal neutron flux in the central experimental hole is given in Figure 31. Data were obtained from Cu-1 percent Au monitor wires placed on a 0.5-inch grid throughout the region at the midplane. A similar plot of the F_1 values, obtained from the same monitors, is given in Figure 32. Corresponding plots for the Mark II fuel element, experimental position are presented in Figures 33 and 34. Values of F_1 along the diagonal of the ARMF-I central experimental hole are also shown in Figure 35. A second curve in the same figure is a plot of F_1 inside a thorium capsule placed at various points along this same diagonal. The significant hardening of the spectrum is due to preferential absorption of thermal neutrons by thorium.

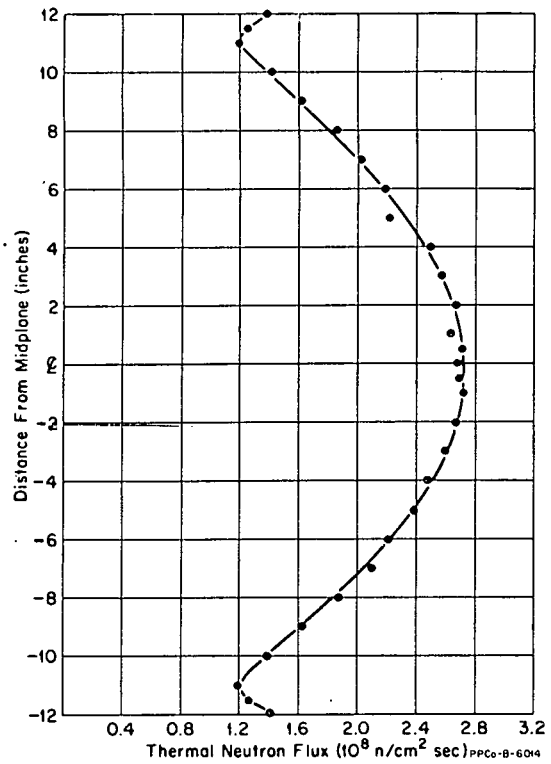

Fig. 27 Vertical distribution of thermal neutron flux in a typical fuel element, ARMF-I.

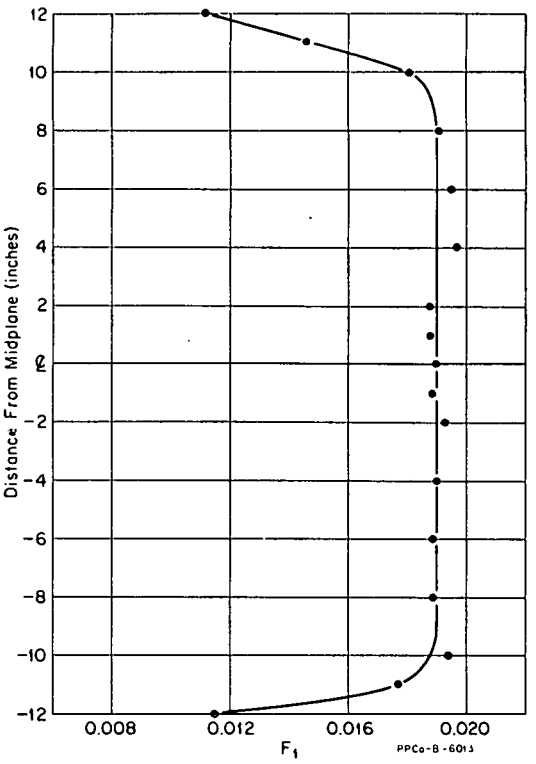

Fig. 28 Vertical distribution of the neutron spectral index in a typical fuel element, ARMF-I.

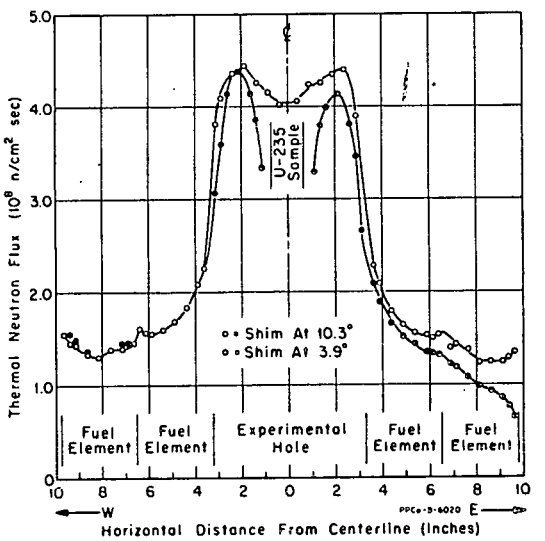

Fig. 29 Horizontal thermal neutron flux distribution at reactor midplane along east-west centerline, ARMF-I.

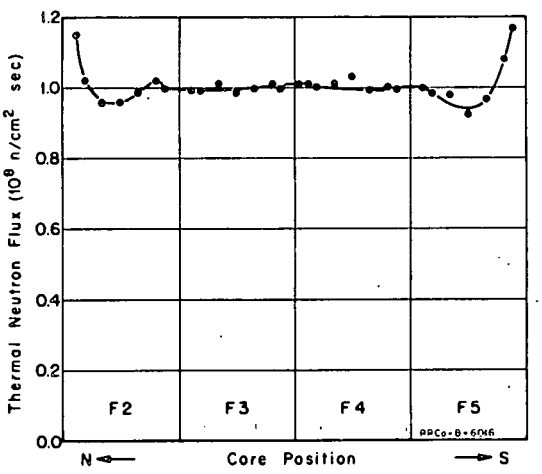

Fig. 30 Horizontal thermal neutron flux distribution at reactor midplane through center of row F fuel elements, ARMF-I.

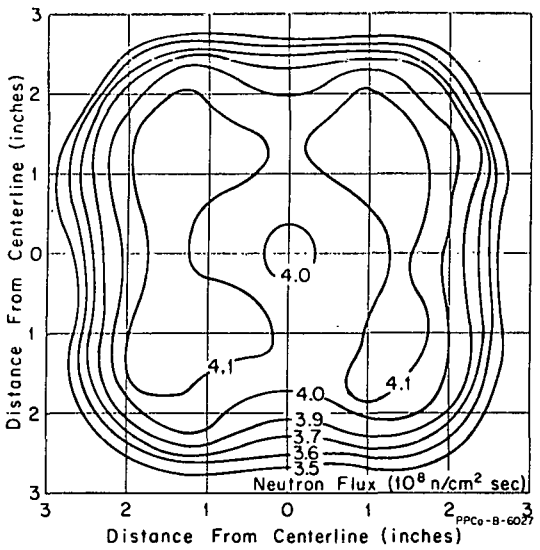

Fig. 31 Contour map of thermal neutron flux in central experimental hole, ARMF-I.

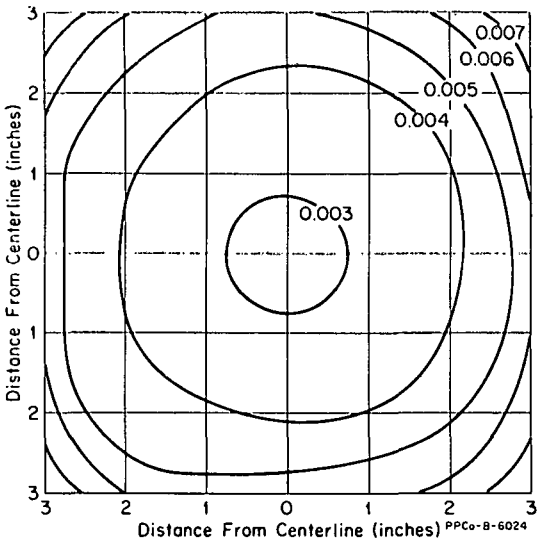

Fig. 32 Contour map of neutron spectral index, F_1, in central experimental hole, ARMF-I.

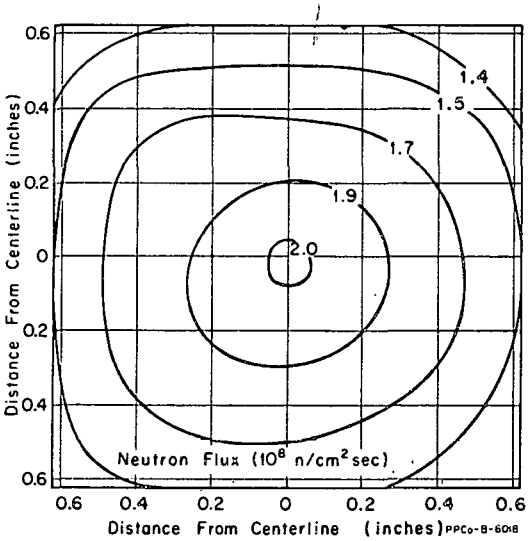

Fig. 33 Contour map of thermal neutron flux in Mark II fuel element experimental hole, ARMF-I.

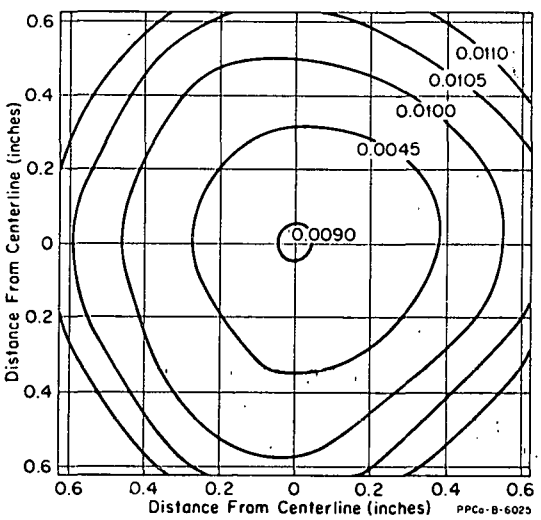

Fig. 34 Contour map of neutron spectral index, F_1, in Mark II fuel element experimental hole, ARMF-I.

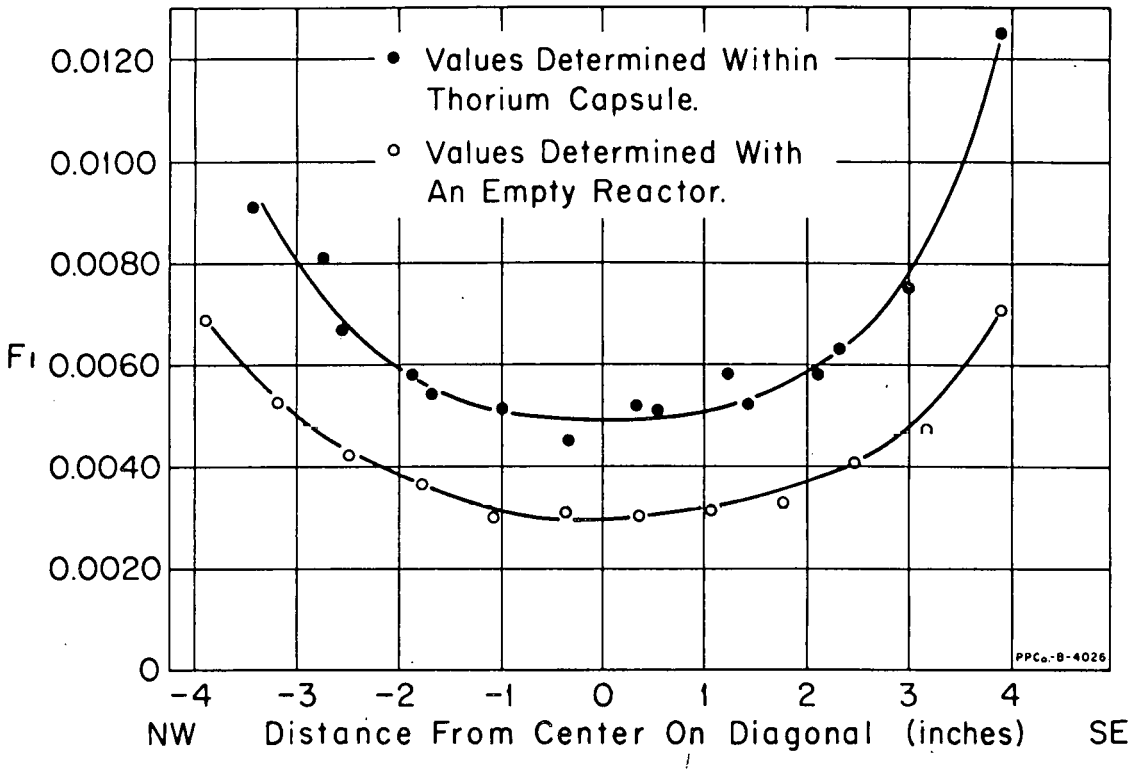

Fig. 35 Traverse of neutron spectral index, F_1, along NW-SE diagonal of central experimental hole, with and without a thorium capsule, ARMF-I.

A vertical flux traverse at the center of the ARMF-I central experimental hole is shown in Figure 36 as having an approximate cosine distribution, symmetric about the midplane. No significant difference in shape was observed for the corner or Mark II element positions. The flux variation over a 6-inch capsule will be less than ± 5 percent when centered at the midplane of the reactor.

1.3 Reflector Neutron Flux Distribution

Flux measurements were made in the reflector, perpendicular to the center of the north face of ARMF-I, using a gold wire 0.04 inch in diameter. Figure 37 shows the thermal flux plot which assumes the characteristic exponential decrease after about three inches with a relaxation length of two inches. (Note that this is somewhat greater than the relaxation length of thermal neutrons in water because the source plane is not thermal.) Higher energy neutrons are fed into the thermal group at all points.

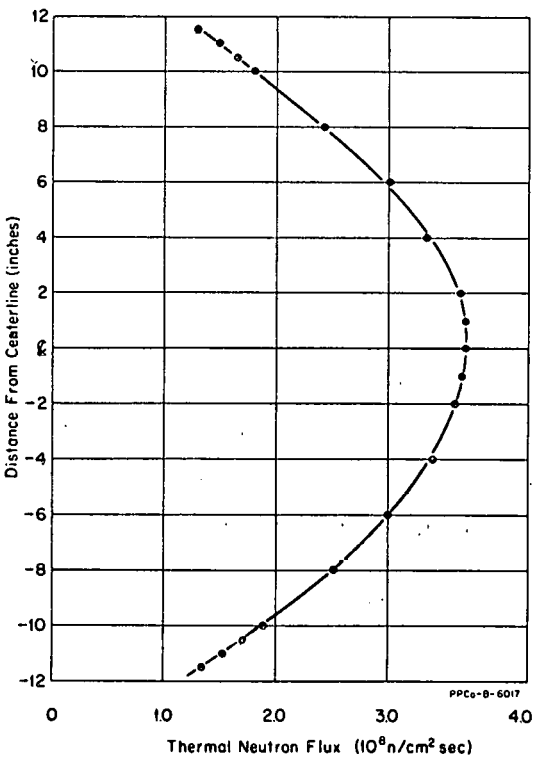

Fig. 36 Vertical thermal neutron flux distribution along the axis of the central experimental hole, ARMF-I.

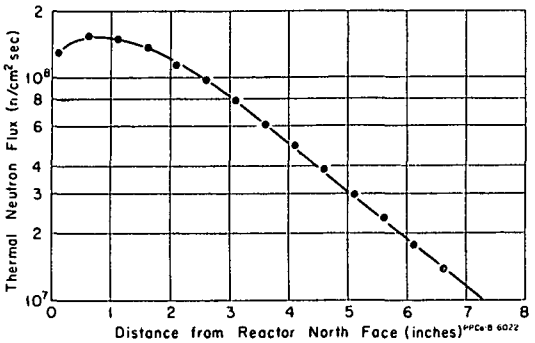

Fig. 37 Thermal neutron flux distribution into water reflector from center of reactor north face, ARMF-1.

The cadmium ratio for the gold wire, using 0.02-inch-thick cadmium, reaches an approximately constant value of 20 at about three inches, also.

2. CONTROL ROD REACTIVITY WORTH

The reactivity worths of the control rods in three different core loadings are listed in Table III. As would be expected, the rod worths are affected significantly by the loading arrangement. The worth of the safety rods and the regulating rod are lower in the two ARMF-II loadings, principally because the rods are not ideally located near the fuel. The lower worth of the shim in the ARMF-II loading is due to its smaller surface area. Even at these lower values, however, the rods have sufficient worth to meet shutdown and capsule measurement requirements.

TABLE III

CONTROL ROD REACTIVITY WORTHS, $\Delta k/k$

Core	Regulating Rod	Shim Rod	Safety Rods
ARMF-I 2-62	0.12 percent	0.73 percent	8 percent - 9 percent
ARMF-II 4-63	0.09 percent	0.45 percent	5 percent - 6 percent
ARMF-II 3-64	0.08 percent	0.36 percent	5 percent - 6 percent

3. TEMPERATURE COEFFICIENTS OF REACTIVITY

Since all measurements conducted to date in the ARMF have need for a constant temperature, only limited experiments have been conducted [10] to determine the reactivity effects due to temperature changes. The temperature coefficients of reactivity for the core and for typical capsules will be presented. The coefficient for a capsule is defined as the change in its reactivity effect on the reactor per unit temperature change of the core (and capsule since it is in the environment of the core).

The response of the ARMF-I core to a temperature change is determined from the regulating rod position during servo operation. The regulating rod position, converted to reactivity units by use of a calibration table, is shown as a function of temperature in Figure 38. The data which cover a range between 17 and 29° C were fitted to a third order power series so that the temperature coefficient could be computed. The temperature coefficient, which is

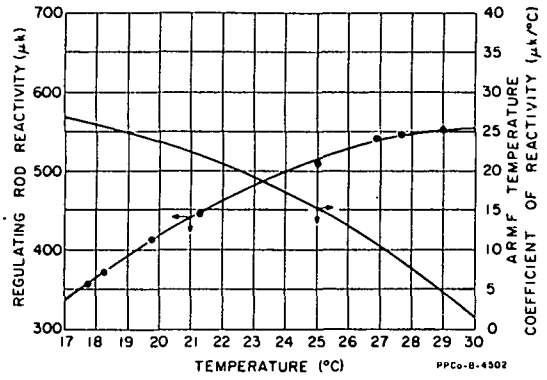

Fig. 38 ARMF-I core temperature coefficient of reactivity.

the slope of this curve at any point, is $d\rho/dT = 15.0 + 2.2\ T - 0.088\ T^2$, where T is the temperature in °C. Thus, at the usual operating temperature of 18°C, the coefficient is 26 μk/°C (μk = 10^{-6} Δk/k). If the curve may be extrapolated, a zero temperature coefficient occurs at about 30.5°C, whereas a maximum of 29 μk/°C is obtained at about 12.5°C. Upon examining the magnitude of the temperature coefficient, it is apparent that the design objectives of a near zero temperature coefficient were achieved with reasonable success.

Figures 39 and 40 show the reactivity worth of an absorptive capsule in two ARMF-I experimental positions as a function of moderator temperature. The temperature coefficient curves, computed from the fitted curves, are also shown in Figures 39 and 40. Whereas the capsule has a negative temperature coefficient in the center position; it has a positive coefficient in the lattice position. It should be observed that in any case the temperature coefficient is rather small. This is a negligible effect, considering that the temperature can be controlled to within ±0.005°C.

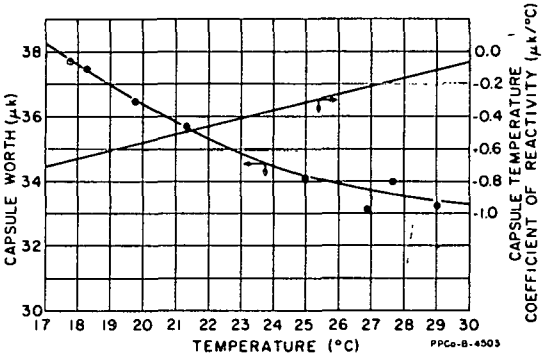

Fig. 39 Capsule A temperature coefficient of reactivity, position 1, ARMF-I.

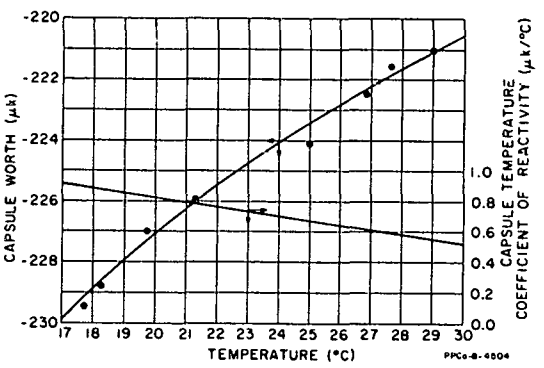

Fig. 40 Capsule A temperature coefficient of reactivity, position 6, ARMF-I.

In Figure 41 similar data for a second capsule are given. This capsule has the same geometry as the first, but has a composition which has a lower absorption cross section and a higher scattering cross section. These data, obtained in the ARMF-I lattice position, show the capsule to have a low, but nearly constant, temperature coefficient over the temperature range considered.

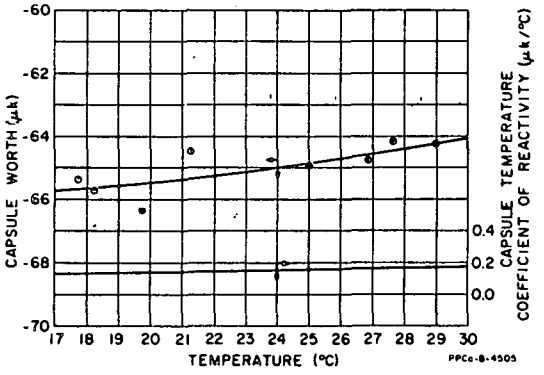

Fig. 41 Capsule B temperature coefficient of reactivity, position 6, ARMF-I.

The foregoing typical examples illustrate that the ARMF-I temperature coefficient is a function of sample material and the experimental position in which the sample is measured. It further illustrates that, in general, one can

expect the temperature effects to be low, particularly in view of the minor temperature changes experienced in actual practice. For precise work, the individual samples should be investigated with respect to their temperature characteristics.

Since the ARMF-II has a close-packed core, its temperature coefficient, measured to be 82 μk/°C at 20°C, is much higher than the ARMF-I coefficient. Insufficient data are available to give the temperature dependence of the core temperature coefficient or the temperature coefficients of capsules.

4. STATISTICAL WEIGHTS

The accuracy with which a measurement is made depends largely on the sensitivity of the measuring instrument. The sensitivity (statistical weights) of three different ARMF loadings to representative materials is presented in Tables IV and V. The core loading arrangements are shown in Figures 12, 13, and 14. The values given in Table V were measured inside a cadmium shield described in Section V-2. It is interesting to note the increase in absorption sensitivities of the small ARMF-II cores over the large ARMF-I core. The statistical weight for boron increased a factor of almost 3.5, producing the very large statistical weight of 28,000 μk/g (or stated more impressively, 2.8 percent/g). The statistical weight for resonance absorption increased a factor of five; whereas, the sensitivity to scattering increased approximately a factor of only two.

TABLE IV

UNSHIELDED INFINITELY DILUTE ABSORPTION SENSITIVITIES

		Material and Reactivity (μk/g)	
Core Loading	Experimental Position[a]	U-235	Natural Boron
ARMF-I 2-62	1	636	-2,688
	3	604	-8,106
	7	175	-7,707
ARMF-II 3-64	1	538	-28,000

[a] Refer to Figures 12, 13, and 14 for core positions.

TABLE V

CADMIUM SHIELDED ABSORPTION AND SCATTERING SENSITIVITIES

Core Loading	Experimental Position[a]	Material and Reactivity (μk/g)		
		Aluminum	Lead	Gold
ARMF-I 2-62	7	0.211	0.064	-22
ARMF-II 4-63	1	0.478	0.085	-116

[a] Refer to Figures 12, 13, and 14 for core positions.

VII. PERFORMANCE CHARACTERISTICS

The precision attained in reactivity measurements is described in this section. Section VII-1 includes a discussion of the data which lead to a value for the servo-loop reactivity noise, interpreted to be the ARMF fundamental limit. Section VII-2 presents the data from measurements conducted to determine the mechanical stability and positioning reproducibility of the core components. Section VII-3 presents data from several ARMF programs which show the achieved reactivity precision of capsule measurements.

The evaluation in this report is an experimental approach; an analytical evaluation will be published later [11].

1. SERVO-LOOP REACTIVITY NOISE

The accuracy with which reactivity measurements can be made is limited by the magnitude of the noise in the system. The system noise is made up of pile noise, chamber (neutron detector) noise, servo electronic noise, temperature noise (drifts), and mechanical noise. The combined effects of all these sources of noise have been measured to determine the limiting precision of reactivity measurements in the ARMF. The parameter to be evaluated is referred to as the ARMF fundamental limit. Before the fundamental limit can be evaluated, however, it is necessary to determine the relative servo performance as a function of reactor power.

Knowing that the accuracy with which reactivity measurements can be made is inversely proportional to the square root of the reactor power [12], but that in practice this relationship does not hold when power-induced temperature effects are experienced, the servo-loop noise was measured as a function of reactor power. The servo gain was also made a variable in these measurements because the optimum gain setting is likewise a function of reactor power. The results of measurements in ARMF-II are shown in Figure 42. Servo operation at gain settings not shown in the figure was either unstable at high gain settings or unresponsive at low settings. It can be seen that optimum operation is experienced in the vicinity of 50 watts. Data from ARMF-I measurements, although less extensive, indicate optimum operations at nearly the same power level.

The data for Figure 42 were obtained by operating the reactor in servo control for extended periods. During these periods disturbances were minimized in the following ways: (a) No capsule measurements were made, (b) the reactor was not mechanically disturbed, except by whatever ground vibration might be transmitted through the vibration absorber pad (Section III-1 and Appendix A), and (c) the canal water temperature was maintained at 18°C $\pm$ 0.002°C. The regulating rod position was sampled at a rate of 16/sec, and the data accumulation time for each IBM card was set at 4.5 minutes (Section IV-2). The data (or cards) were analyzed with a standard ARMF computer program which computes an average rod position for each card and a standard deviation of the eight subaverages. To gather a sufficient number of card averages to obtain meaningful statistics, ten cards were run in succession. The standard deviations from all cards were then averaged to obtain a statistically significant standard

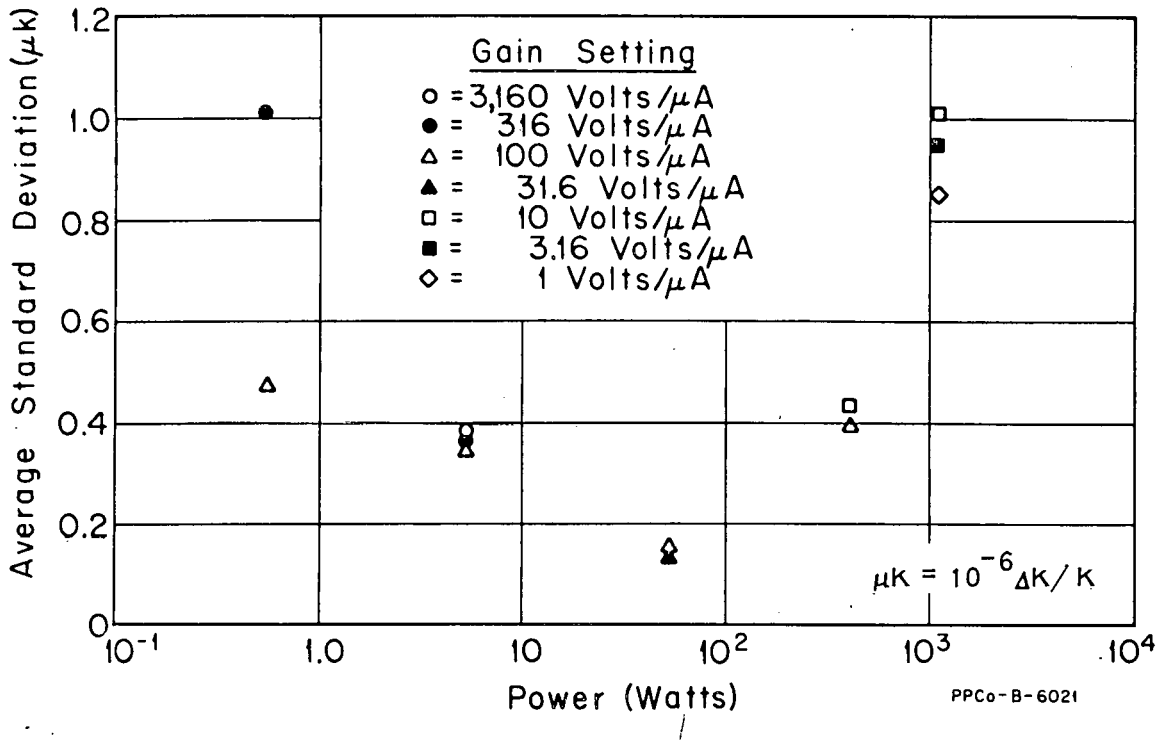

Fig. 42 Regulating rod noise as a function of reactor power and servo amplifier gain.

deviation for a given condition. The data analysis is described mathematically in the following.

A_{ij} = average rod position during jth subinterval of the ith card.

$$A_i = 1/8 \sum_{j=1}^{8} A_{ij} \text{ - average rod position during ith card.}$$

$$s_i = \frac{1}{\sqrt{8-1}} \left\{ \sum_{j=1}^{8} (A_{ij} - A_i) \right\}^{\frac{1}{2}}$$

$$\bar{s} = 1/10 \sum_{i=1}^{10} s_i$$

It is to be noted that the subaverages are not completely independent; however, the data are to be compared on a relative basis, and therefore no loss of meaning is incurred.

The fundamental limit for both ARMF-I and -II, operating at the optimum power (≈50 watts) will now be evaluated. As in the previous study, the reactor was operated in servo control with no disturbances during which time the averaged

regulating rod position was continuously punched into IBM cards. The canal temperature during this period was controlled between the limits shown in Table VI, which also includes the results of this study. Under these conditions, ARMF-I experienced no detectable reactivity drift, whereas ARMF-II experienced a linear reactivity drift of 1.2 μk. Because ARMF-I experienced no drift, the standard deviation of the rod motion was obtained as follows:

A_i - Average rod position during interval of ith card

$$A = \frac{1}{N} \sum_{i=1}^{N} A_i$$

$$s = \frac{1}{\sqrt{N-1}} \left[\sum_{i=1}^{N} (A_i - A)^2 \right]^{\frac{1}{2}}$$

where s is the estimated standard deviation, and N is the number of cards punched. Because capsule measurements are made for a duration of 270 sec, card averages, rather than subaverages, are used in this analysis. ARMF-II data were treated in a similar manner, but, because of the reactivity drift, the data were treated in a manner which is analogous to the method of drift corrections during actual capsule measurements. The card averages were fitted to a straight line and the deviations, corresponding to $(A_i - A)$, were obtained from the differences between A_i and a point on the line corresponding in time to the midpoint of the ith card.

The results of both analyses are shown in Table VI. An F test, at a significance level of five percent applied to the data from both reactors, requires an acceptance of the hypothesis that there is no real difference between ARMF-I and ARMF-II servo operation.

TABLE VI

ARMF-I AND ARMF-II SERVO-LOOP NOISE ANALYSIS

	Temperature (°C)	Number of Cards (N)	Durations of Run (minutes)	Standard Deviation (μk)
ARMF-I	18.000-17.998	18	81	0.068
ARMF-II	17.997-18.002	24	108	0.084

It is interesting to compare the standard deviation, or statistical errors listed in Table VI, to the "fundamental statistical errors in criticality measurements" predicted by Cohn [12], which are errors due to pile noise. In this work, it was found that the limiting error could be expressed as follows:

$$s(t) = 5.1 \times 10^{-6}/\sqrt{Wt}$$

where W is the reactor power in watts, and t is the measuring time in seconds.

Accordingly, the error due to pile noise for conditions of the ARMF measurements [a] is as follows:

$$s(270 \text{ sec}) = 5.1 \times 10^{-6}/\sqrt{50 \text{ W} \times 270 \text{ sec}}$$

$$= 4.38 \times 10^{-8} \ \Delta k/k$$

Comparing this value to the ARMF values indicates that the ARMF fundamental limit is within a factor of two of the fundamental limit due to pile noise.

2. REACTIVITY REPRODUCIBILITY OF CORE COMPONENTS

The accuracy with which reactivity measurements can be made in any reactor is affected by the ability of the mechanical parts to remain fixed, relative to one another when intended (mechanical stability), and by the ability of the parts to return to their intended position when movement is necessary. As was discussed in the design description, all parts in the core are designed to be located precisely and held in place firmly. In the case of the safety rods where free fall due to the force of gravity is required, they were designed to cause a very small reactivity effect when imprecise positioning occurs. Although movements of core components, especially between capsule measurements, have indirect effects on capsule reactivity measurements and are usually of second order, they could become significant when very accurate and precise measurements are necessary. This could occur because statistical weights and rod worths could be changed if the effects are large. In order to determine the mechanical stability and positioning reproducibility of the ARMF, the reactivity reproducibilities for various disturbances were measured. The results of these measurements are shown in Table VII. The number of degrees of freedom for each measurement depended upon the difficulty of the measurement and the importance of the results. For example, only four measurements were made on upper grid removal. For all of these measurements, the temperature was controlled to $\pm$ 0.005°C. It can be seen in the table that the largest effect, 12 μk, is due to upper grid removal (corresponding to core disassembly), which is a small effect for such a major disturbance. Since the effects listed in the table are second order effects, they should have a very small effect on capsule reproducibility.

3. REACTIVITY REPRODUCIBILITY OF CAPSULE MEASUREMENTS

The reproducibility, or precision, of capsule measurements is influenced by many effects: (a) capsule design, (b) capsule holder design, (c) experimental

[a] Chamber efficiency is approximately 10^{-4} in the ARMF. According to Cohn this is large enough not to be a limiting factor.

TABLE VII

REACTIVITY REPRODUCIBILITY OF REACTOR SYSTEMS

Cause	Degrees of Freedom	Standard Deviation (μk)
Scram	9	1.2
Scram and Universal Capsule Holder Removal	6	4.7
Upper Grid Removal	3	12.1
Safety Rod Upper Limit	8	0.23
Shim Rod Position	8	0.24

position, and (d) time duration of the measurements. These are all in addition to the fundamental limit (discussed in Section VII-1) determined by servo-loop noise (including pile noise). Data regarding the reproducibility of capsule measurements have been collected from several ARMF programs for the purpose of evaluating these effects. A summary of the data to be discussed is given in Table VIII. All capsule measurements selected were made for 4.5 minutes, and empty reactor measurements of the same duration were made following every three of four capsule readings. A capsule reactivity worth is the difference between the reactivity values (from the regulating rod calibration) which correspond to the average rod position during the capsule and empty measurements. The empty rod position is a time interpolation of those empty rod positions measured before and after the capsule measurement.

The data in Table VIII have been grouped according to reactor, capsule, type, and experimental position. Where a range of capsule worths is indicated, the standard deviation was calculated by combining the data in the following manner:

$$s = \frac{1}{\sqrt{N-K}} \left[\sum_{j=1}^{K} \sum_{i=1}^{N_j} (X_{ij} - \bar{X}_j)^2 \right]^{\frac{1}{2}}$$

where

X_{ij} is the ith measurement of the jth capsule

$\bar{X}_j$ is the mean worth of the jth capsule with N_j measurements

N is the total number of measurements, and

K is the total number of capsules.

TABLE VIII

MEASUREMENT ERRORS FOR SEVERAL CAPSULE TYPES

Capsule Type	Experimental Position	Degrees of Freedom	Type of Measurement	Capsule Worth (μk)	Standard Deviation[a] (μk)
			ARMF-I		
A	1	162	1	0-200	0.13
A	1	36	1	200-500	0.17
A	1	249	1	93-305	0.13
A	1	8	2	295	0.43
C	1	16	1	61	0.10
C	1	72	1	119-590	0.28
C	7	27	1	420	0.28
C	7	20	1	15.2	0.20
C	5	20	1	367	0.29
D	1	30	1	692	0.20
D	1	50	2	692	0.30
D	3	50	2	358	0.70
			ARMF-II		
A	1	162	1	237-512	0.19
C	1	58	1	95	0.35
H	1	660	1	7-400	0.24

[a] Time for each measurement is 4.5 minutes.

Listed in the table are measurements of two types. A Type-1 series of measurements is one that can be completed in one day, whereas a Type-2 series is one in which the measurements are spread over a period of several days to a few years. Measurements of the Type-1 class are cross section and resonance integral measurements. Measurements of the Type-2 class are those on capsules requiring long-term irradiation programs in the MTR or ETR. The Type-1 measurements are made without reactor disturbances. Interspersed among Type-2 measurements are various disturbances: reactor scrams and shutdowns, capsule holder removals, and possibly core disassembly if reactor repairs below the grids are required.

Type-1 measurements in ARMF-I will be discussed first. In general, it is seen that the standard deviations for measurements made in the center of ARMF-I (position 1) are smaller than those for other positions. This is the case because the flux gradient in this position is nearly zero (Section VI-1.2); therefore, a displacement of the capsule, due to inaccurate positioning, causes a very small reactivity effect. The standard deviation of 0.28 for the one set of Type-C capsules in position 1 seems anomalously large and is not fully understood; the reason for the large value is currently under study. It can be seen in the table that there are larger, but only slightly larger, errors associated with measurements in positions other than the center. This is attributed to the flux gradients

in these positions. Even a slight variation in the position of the capsule from one measurement to the next causes a variation in its reactivity worth.

The errors of Type-1 measurements in ARMF-II are comparable to those for ARMF-I. Although the experimental position in ARMF-II is located at the approximate center of the core, flux gradients do exist and position accuracy is important. This is reflected in the Type-C capsule data. The materials in these capsules are not completely homogeneously dispersed; therefore, changes in orientation of the capsule change its worth which appears as a larger error.

The errors for three Type-2 measurements are presented in Table VIII. It is seen that they are large compared to Type-1 measurement errors. In fact, one set of values can be compared directly because they are from the same capsule measured under both conditions. The data are identified by the capsule worth of 692 μk. The larger errors, associated with Type-2 measurements, are attributed to statistical weight changes, when capsule holders do not return precisely to their original positions, and possible changes in regulating rod calibrations. It is to be noted that the canal temperature during the time of measurements was 18°C ± 0.005°C. Without close temperature control, much larger errors would be experienced. It is interesting to compare the actual precisions listed in Table VIII to the limiting precision due to servo-loop noise (Table VI). Since each capsule reactivity worth is based on one capsule measurement and two empty (reactor) measurements, the limiting precision for a capsule worth will be different than the fundamental limit of a single measurement. The limiting precision is obtained as follows:

$$\Delta\rho = \frac{\rho_{e1} + \rho_{e2}}{2} - \rho_c$$

where

$\Delta\rho$ is the reactivity worth of the capsule

ρ is a value from a regulating rod reactivity calibration

c denotes capsule, and

e1 and e2 denote empty measurements.

In actual reactivity measurements, the ρe's are time interpolated which is not necessary for this development. The error, or standard deviation, in the net reactivity measurement would then be:

$$s_{\Delta\rho} = \left[\frac{s_{e1}^2}{4} + \frac{s_{e2}^2}{4} + s_c^2\right]^{1/2}$$

or

$$s_{\Delta\rho} = \sqrt{\frac{3}{2}}\, s_e = 1.225 \times 8.4 \times 10^{-8} = 0.105 \quad \mu k$$

when s_e and s_c are assumed to be equal to the fundamental limit, s, obtained in Section VII-1.

VIII. REFERENCES

1. W. E. Nyer et al, Proposal for a Reactivity Measurement Facility at the MTR, IDO-16108 (August 1953).

2. J. W. Webster, A Critical Assembly Having Maximum Sensitivity, IDO-16248 (August 1953).

3. D. R. deBoisblanc et al, "The Reactivity Measurement Facility and Its Applications" in Proceedings of the Second United Nations International Conference on the Peaceful Uses of Atomic Energy held in Geneva September 1 - 13, 1958, A/CONF. 15/P/1842.

4. R. S. Marsden (unpublished).

5. T. E. Cole et al, The MTR Safety System and Its Components, ORNL-1139 (April 1952).

6. J. B. Ruble and S. H. Hanauer, Testing Procedures for Reactor Instrumentation. Section P. Composite Safety Amplifier (Q-1565), CF-56-5-30 (Section P) (March 1955).

7. R. I. Little, ARMF-II Regulating Rod Readout and Shim Rod Drive and Position Display, IDO-16896 (September 1963).

8. R. G. Nisle, "A Unified Formulation for the Specification of Neutron Flux Spectra in Reactors", in Neutron Dosimetry. Vol. 1. Vienna, IAEA, 1963 pp 111-52.

9. C. H. Westcott, "The Specification of Neutron Flux and Nuclear Cross-Sections in Reactor Calculations", J. Nuclear Energy 2, No. 1 (August 1955) pp 59-76.

10. J. W. Rogers et al, "Temperature Effects in the ARMF" in MTR-ETR Technical Branches Quarterly Report, 3rd Quarter 1962, IDO-16827 (January 1963) pp 3-5.

11. L. G. Cloud et al, ARMF-II Noise Study, IDO-16959 (1964) (unpublished).

12. C. E. Cohn, "A Simplified Theory of Pile Noise", Nuc. Science and Engineering, 7 (May 1960) pp 472-75.

13. D. H. Gipson, "Calibration of the ARMF-I and ARMF-II Regulating Rods" in MTR-ETR Technical Branches Quarterly Report 4th Quarter 1963, IDO-16977 (May 1964) pp 58-61.

APPENDIX A

EFFECTIVENESS OF PARAPET-CONTROL BRIDGE VIBRATION ABSORBER

THIS PAGE

WAS INTENTIONALLY

LEFT BLANK

APPENDIX A

EFFECTIVENESS OF PARAPET-CONTROL BRIDGE VIBRATION ABSORBER

A vibration absorbing material is positioned between the ARMF control bridge and the canal parapet. The purpose of this material, Johns-Manville "Spintex" Type-413 fiber glass insulation, is to isolate the ARMF from building and ground vibrations. To determine the effectiveness of the isolation, the amplitude and frequency of vibrations were measured on the ARMF-I control bridge and the canal parapet.

A General-Radio vibration meter (Type 761-A) was used to measure the amplitude of the vibrations, and a General-Radio sound analyzer (Type 760-B) was used to measure the frequency.

Vibration measurements were made while the ARMF, the large air compressors (located outside the ARMF building), and the canal stirrers were operating. In order to determine the source of the vibrations, measurements also were made with the canal stirrers turned off, since it was believed they would be the primary source of any vibrations. This assumption proved to be true because vibrations, even on the parapet, were not detected with the canal stirrers turned off.

The measurements with the canal stirrers turned on are summarized in Table A-I. These measurements show that the insulation material effectively isolates the ARMF from vibrations which would otherwise be transmitted through the parapet.

TABLE A-I

ARMF VIBRATION MEASUREMENTS

Measurement Location			
Control Bridge		Canal Parapet	
Frequency (cps)	Amplitude (micro inch)	Frequency (cps)	Amplitude (micro inch)
58	not measurable	29	28
		58	64
		120	13
		175	6
		290	3

THIS PAGE

WAS INTENTIONALLY

LEFT BLANK

APPENDIX B

ARMF-I REGULATING ROD BEARING DIFFICULTIES

THIS PAGE

WAS INTENTIONALLY

LEFT BLANK

APPENDIX B

ARMF-I REGULATING ROD BEARING DIFFICULTIES

Following the second year of ARMF-I operation, occasional binding in the regulating rod bearing was experienced. Although the binding was sufficient to stop the rod, the rod could be freed by rotating it by hand. On August 7, 1963, the reactor was shut down to inspect the lower regulating rod bearing and to make other miscellaneous repairs.

The lower bearing of the regulating rod consists of a tungsten carbide raceway, five tungsten carbide balls, and the conical Carbaloy lathe tip which formed the lower end of the rod. The balls were spaced by a Teflon retainer. Figure B-1 shows the details of this assembly.

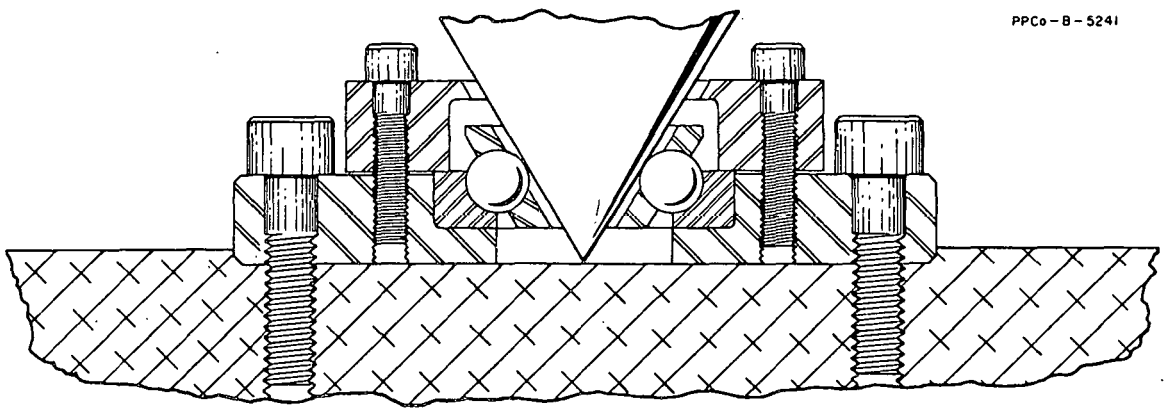

Fig. B-1 Original ARMF lower bearing assembly.

When the regulating rod was removed from its lower bearing, it was found that the Teflon retainer had become distorted and that the five tungsten carbide balls had worn considerably. The maximum change on the ball diameters was between 4.8 and 6.8 mils. From the condition of the retainer, it appears that the balls tended to ride on the retainer and thus drag, causing the balls and conical tip to wear. Figure B-2 is a photograph of the used and new Teflon retainers, ball bearings, and Carbaloy lathe tips.

The bottom bearing of the regulating rod was replaced with a new Carbaloy lathe tip, new tungsten carbide ball bearings, and a modified retainer to prevent the tendency for the balls to ride on the retainer. The thickness of the retainer was increased from 0.040 inch to 0.115 inch and the material was changed to 304 stainless steel.

The new retainer is believed to be only a partial solution, and the bearing as reinstalled was only an expedient means of getting the reactor back in service. In addition to the retainer problem, the point contact between the lathe tip and the balls probably produces excessive loading and, thus, excessive wear. Excessive wear, caused by corrosion, has been ruled out because the

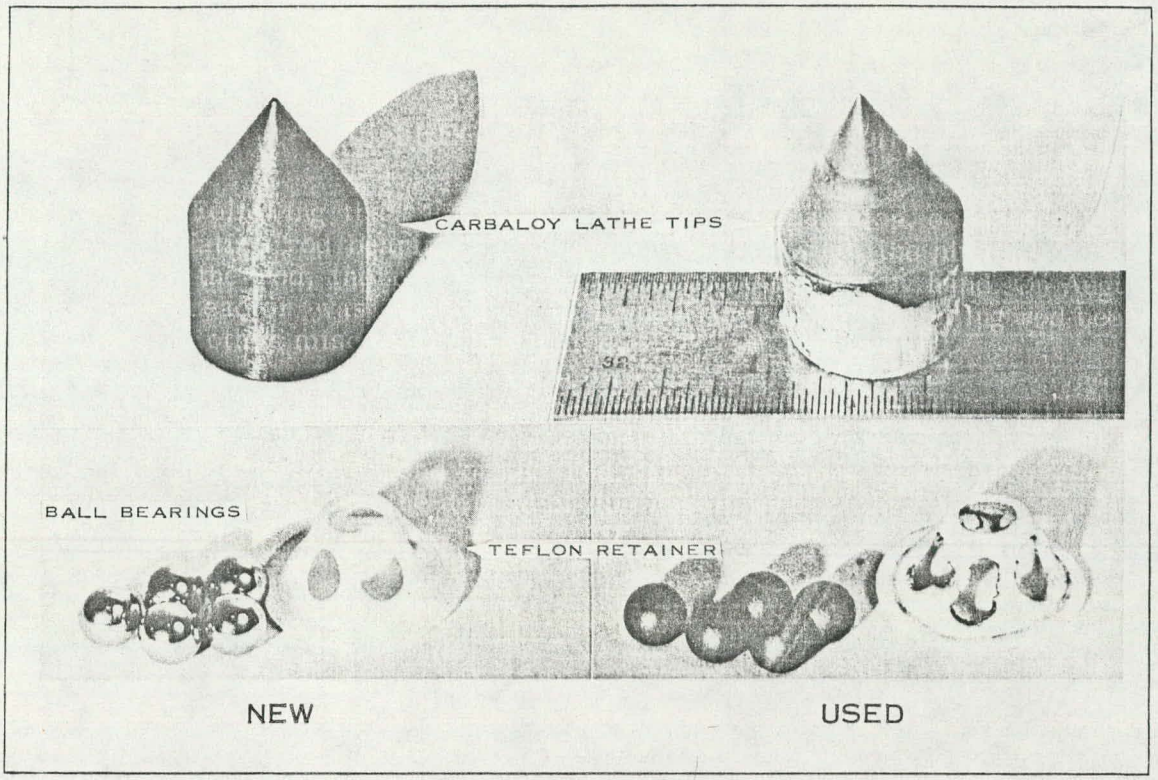

Fig. B-2 ARMF lower bearing components.

pH of the canal water is maintained between 5.5 and 6.5. Since disassembly of the core for regulating rod bearing repairs introduces possible changes in statistical weights and calibrations, the bearing has been redesigned as shown in Figure B-3.

In the new design the number of ball bearings has been increased from 5 to 16 which has eliminated the need for a ball retainer. To eliminate the point contact on the balls, the lathe tip has been replaced with a conventional raceway. The ball bearings are made of Stellite No. 3 with a diameter of 0.1875 inch, and the raceways are made of Stellite No. 19.

Although the new bearing is expected to operate for many years without difficulty, the entire bearing is designed to be attached to the bottom of the regulating rod so that it can be removed with the regulating rod without draining the canal.

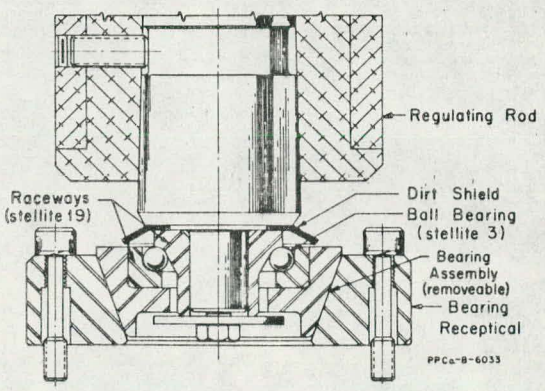

Fig. B-3 Redesigned ARMF lower bearing assembly.

APPENDIX C

REGULATING ROD CALIBRATION PROCEDURE

THIS PAGE

WAS INTENTIONALLY

LEFT BLANK

APPENDIX C

REGULATING ROD CALIBRATION PROCEDURE

The accuracy of ARMF reactivity measurements depends upon an accurate reactivity calibration of the regulating rod. A new technique of calibration was developed for use in the RMF, which with subsequent modifications, is still used for calibrating ARMF regulating rods. Several conventional methods had been considered, but were discarded because they required too much time to give the required accuracy. They are used to some extent, however, to check the validity of calibrations by the new technique.

The calibration is done in two steps: (a) measurements are made which will define the relative shape of the calibration curve; and (b) data from these measurements are fitted to a functional relationship, and period measurements are taken to scale the curve to absolute reactivity values.

1. MEASUREMENTS USED TO DEFINE RELATIVE SHAPE

With the shim rod adjusted so that the regulating rod is near its lower limit, the regulating rod position is determined with a capsule [a] in and out of the reactor. The shim is then inserted to cause the regulating rod to withdraw slightly, and a second set of capsule in and out measurements are made. This procedure is repeated until the entire span of the regulating rod has been covered. All that is left to complete the calibration is to fit these pairs of values to a functional relationship and to scale it to the reactivity worth of the rod. Before discussing the fitting and scaling procedure (Section C-2), however, it is appropriate to discuss measurements which have been made to determine the validity of this calibration procedure.

Three conditions must exist for this calibration method to be useful. (a) The movements of the shim rod must not affect the shape of the calibration curve; (b) the true reactivity worth of the calibration capsule must be a constant for all regulating rod positions; and (c) the worth of a capsule must be the same at different rod positions, regardless of the magnitude of its reactivity worth.

To determine that the shim movement did not cause a localized perturbation which would affect the curve shape, two separate calibrations were made and compared. For the first calibration, the regulating rod was adjusted by moving the shim rod. For the second calibration, the rod position was adjusted by inserting poison wires uniformly throughout the reactor while the shim remained in a stationary position. When the two calibration curves were compared it was found that, within the accuracy of the measurements, the shape remained the same.

---

[a] To be able to cover the entire regulating rod, the capsules reactivity worth must be less than half the worth of the regulating rod.

To determine that the reactivity worth of the calibration capsule is a constant for all regulating rod positions, period measurements were used to determine the capsule worth at several different regulating rod positions. The measurement was repeated several times at each position to obtain an accuracy which showed that with a confidence level of 90 percent, the reactivity worth of the calibration capsule did not change more than 1 μk for an assumed Student "t" statistical level of 5 percent.

To determine that the calibration will give a constant reactivity worth to a capsule regardless of its reactivity worth, two capsules with different reactivity worths (≈100 μk and ≈ 500 μk) were measured at several different regulating rod positions. An analysis of the data showed that there was no statistically significant variation in the capsule worth.

After determining from the experiments and studies just described that the method used to obtain the calibration curve was valid when only one experimental position is involved, additional studies were conducted to determine if a calibration obtained from capsule measurements in one experimental position applies with equal accuracy to other experimental positions. Comparisons of two different sets of data were made to test the application of the curve to different experimental positions. The first comparison was made by use of data from two independent calibrations. Two calibration curves were obtained for the same capsule measured in two different positions (1 and 7) in ARMF-I. The reactivity worth of the calibration capsule was then determined from both calibrations in both positions, producing four sets of data. The standard deviations of the capsule worth for each of the four sets of data are listed in Table C-I. It can be seen that when the capsule measurements and the calibration are made in the same position the standard deviation is small, as would be expected, since these standard deviations are of the residuals of the calibration curve fitting (Section C-2). However, when the calibration and the capsule measurements are made in different positions, the standard deviation is significantly higher as seen in the table. To determine if there is a correlation between the increased error and regulating rod position, the data for measuring position 7 and two calibration curves were plotted as shown in Figure C-1. It can be seen that when the calibration for position 1 is used the capsule value varies systematically as a function of the regulating rod position; and that for a capsule of this worth (73 μk), the deviation is approximately 1 μk near the limits.

TABLE C-I

MEASURING AND CALIBRATION POSITION COMPARISON

Measuring Position	Calibration Position	Standard Deviation (μk)	Capsule Reactivity Worth (μk)
7	7	0.27	73
7	1	1.12	73
1	1	0.24	150
1	7	3.22	150

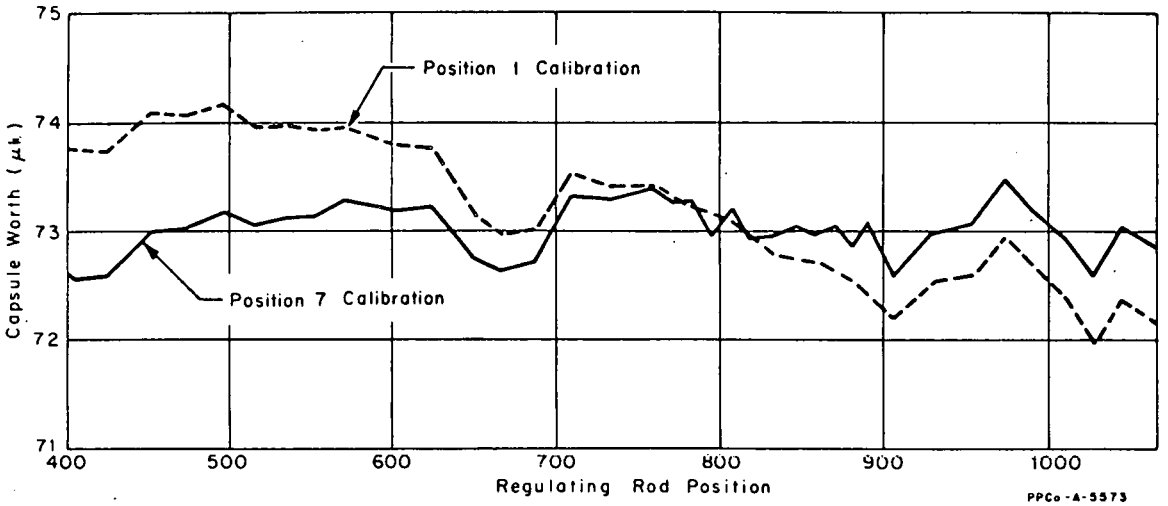

Fig. C-1 Comparison of results of ARMF measuring position calibrations.

The second comparison to check calibration validity involved an analysis of similar, but independent, data measured at different positions of the regulating rod and in two different measuring positions. The reactivity worth of the two capsules as determined from a position 1 calibration are plotted against the regulating rod position in Figure C-2. Plots of data from positions 1 and 4 are included for comparison (Figure C-2). Again it is seen that there is no significant dependence when the experimental and calibration positions are the

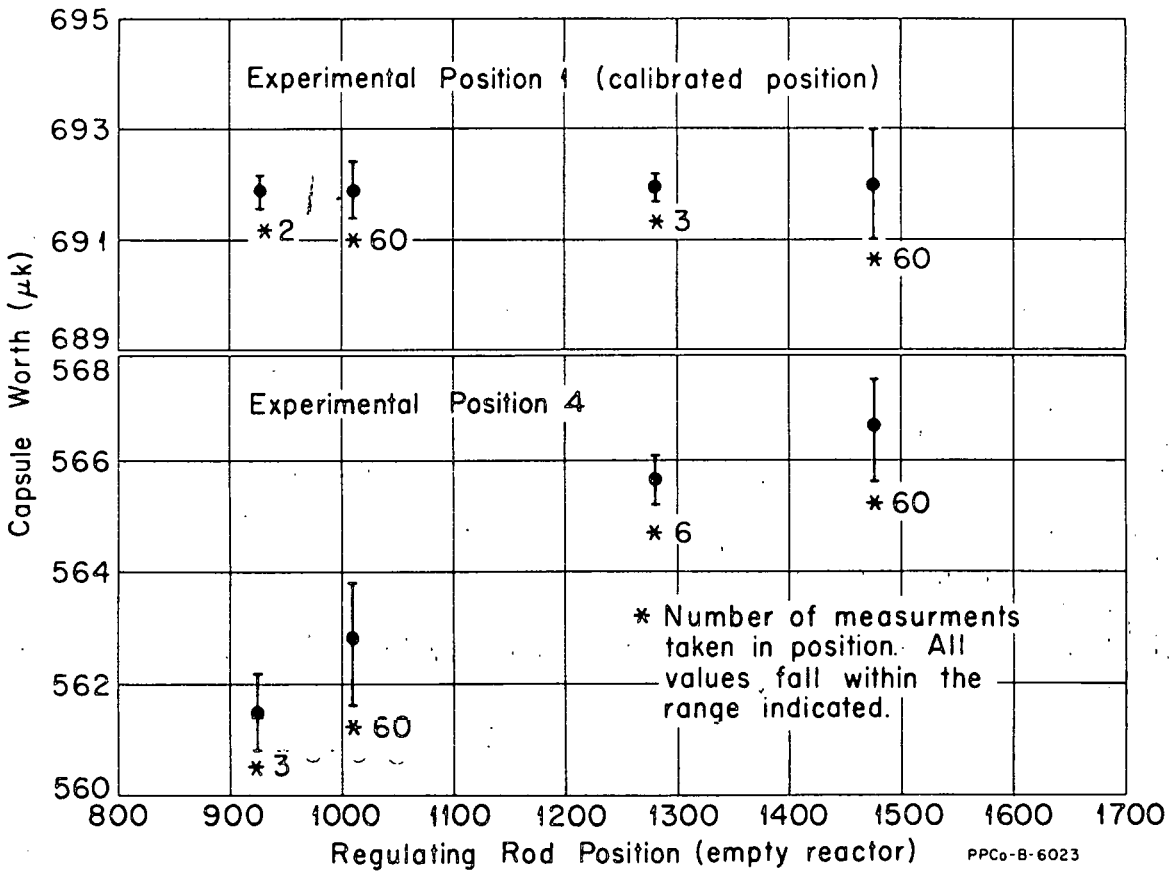

Fig. C-2 Apparent capsule reactivity worth at different regulating rod positions and in two experimental positions.

same, but that a significant dependence exists when the positions are not the same. The apparent worth of the capsule changed by more than 5 μk, even though these data cover only half the total span of the regulating rod.

From the results presented above, it is apparent that for precise measurements the regulating rod must be calibrated for each experimental position used. The error in the calibration when the calibration and measurement positions are not the same is no doubt due to a flux distribution perturbation caused by the interaction of the shim and regulating rods. The fact that there is an effect on the calibration when two positions are used suggests that there may also be a small effect, not detected by the described tests in the foregoing, even when only one position is used. The study of possible effects is continuing.

2. CURVE FITTING AND ABSOLUTE REACTIVITY MEASUREMENTS

A least squares technique, developed by Gipson [13], is used to obtain a functional relationship between reactivity and regulating rod position.

Assuming the true function to be a $\rho = f(r)$, where r is the position of the regulating rod and ρ is the integrated reactivity, an approximating function, $\rho_n = F_n(r)$, is found such that the functional difference, f(r) and $F_n(r)$, is as small as possible. The relative reactivity worth of the calibration capsule is assigned a constant value over the entire range of the regulating rod.

Let

$\Delta\rho$ = an assigned relative reactivity worth of the capsule

r_2^j = regulating rod position with the capsule "in"

r_1^j = regulating rod position with the capsule "out"

Then

$$\Delta\rho = f(r_2^j) - f(r_1^j) \tag{1}$$

for m pairs of readings, j = 1, 2 ..., m.

From the approximating function

$$\rho_n = F_n(r) = a_o + a_1 G_1(r) + a_2 G_2(r) + \ldots + a_n G_n(r) \tag{2}$$

the values of the coefficients, a_i (i=1, 2, ..., N), are found so that the function

$$\Delta\rho_n^j = F_n(r_2^j) - F_n(r_1^j) \tag{3}$$

is a good fit to the experimental values, (r_2^j, r_1^j) and $\Delta\rho$. The method of least squares is used to evaluate the coefficients where the function to be minimized is

$$H(a_1, a_2, \ldots, a_n) = \sum_{j=1}^{m} (\Delta\rho_n^j - \Delta\rho)^2 \tag{4}$$

Polynomial and trigonometric functions have been tried. To date, the trigonometric function shown below usually has given the smallest residuals.

$$\rho\,(r) = a_o + \sum_{k=1}^{n} a_k \sin k\,\theta + \sum_{k=1}^{n} b_k \cos k\,\theta \qquad (5)$$

To be compatible with the binary position instrumentation and provide a convenient scale, the ARMF regulating rod travel has been divided into 1600 divisions. The value of a_o is determined by setting ρ_n equal to zero at r = 1600 which is the upper limit of the regulating rod [a]. θ from Equation 5 is equal to $\frac{\pi r}{1600}$.

The arbitrary value $\Delta\rho$, assigned to the calibration capsule, produces an unnormalized calibration curve. The calibration curve is normalized to an absolute reactivity by measuring the total worth of the rod by repeated period measurements.

[a] Zero has been assigned to the upper limit of the rod so that the empty reactor reading, subtracted from the capsule reading, will give the correct algebraic sign to the capsule worth.

PHILLIPS PETROLEUM COMPANY

ATOMIC ENERGY DIVISION

has been assigned to the upper limit of the rod so that the empty re-
actor reading, subtracted from the capsule reading, will give the correct ir-
radiation capsule worth.